by computational simulation (8, 9). There are four anti-parallel β-sheets involving the N and C termini of both monomer subunits and they contribute close to 75% of the dimerization energy (10), explaining at least in part why DRV failed to dissociate mature protease dimer (see below). The termini interface has been explored as a dimerization inhibition target by several groups (11–13). We have also recently reported that certain peptides containing the dimer interface sequences amino acids 1–5 and amino acids 95–99 blocked HIV-1 infectivity and replication (14). However, to the best of our knowledge, no evidence of direct dimerization inhibition by such compounds has been yet documented.

In the present study, we developed an intermolecular fluorescence resonance energy transfer (FRET)-based HIV-1-expression assay that employed cyan and yellow fluorescent protein-tagged HIV-1 protease monomers. Using this assay, we identified a group of non-peptidyl small molecule inhibitors of HIV-1 protease dimerization. These inhibitors, including the recently approved protease inhibitor (PI) darunavir (DRV) as well as two experimental protease inhibitors, blocked protease dimerization at concentrations of as low as 0.01 μM and blocked HIV-1 replication *in vitro* with $IC_{50}$ values of 0.0002–0.48 μM. These agents also inhibited the proteolytic activity of mature HIV-1 protease. Another PI, tipranavir (TPV), active against HIV-1 variants resistant to multiple PIs, also blocked protease dimerization, although all other existing FDA-approved anti-HIV-1 drugs examined in the present study failed to block the dimerization. The present report represents the first demonstration that non-peptidic small molecule agents can disrupt protease dimerization.

## EXPERIMENTAL PROCEDURES

*Generation of FRET-based HIV-1 Expression System*—CFP- and YFP-tagged HIV-1 protease constructs were generated using BD Creator™ DNA cloning kits (BD Biosciences, San Jose, CA). First, XhoI/HindIII fragments from pCR-XL-TOPO vector containing the HIV-1 protease-encoding gene excised from pHIV-$1_{NL4-3}$ was inserted into the pDNR-1r (donor vector) that had been digested with XhoI and HindIII. In the transfer of the protease gene from the donor vector into pLP-CFP/YFP-C1 (acceptor vector), the Cre-loxP site-specific recombination method was used according to manufacturer's instructions. Using Cre-recombinase with the lox P site, the protease gene from pDNR-1r was inserted into pLP-CFP-C1 or pLP-YFP-C1 through Cre-mediated recombination (15), generating a plasmid of CFP-tagged PRwt and that of YFP-tagged $PR_{WT}$, with which HIV-1 protease was successfully expressed as a fusion protein with CFP- and YFP-tagged at the C terminus, respectively. Western blot assay using anti-green fluorescent protein-specific rabbit polyclonal antibodies revealed that protease was correctly tagged to CFP or YFP (data not shown).

For the generation of full-length molecular infectious clones containing CFP- or YFP-tagged protease, the PCR-mediated recombination method was used (16). To this end, we amplified an upstream proviral DNA fragment containing ApaI site and HIV-1 protease (excised from pHIV-$1_{NL4-3}$) with a primer pair: Apa-PRO-F (5′-TTG CAG GGC CCC TAG GAA AAA GG-3′) plus PR-5Ala-R (5′-GGC TGC TGC GGC AGC AAA ATT TAA AGT GCA GCC AAT CT-3′), a middle proviral DNA fragment containing CFP (excised from pCFP-C1) or YFP (excised from pYFP-C1) (Clontech, Mountain View, CA) with a primer pair: CFPYFP-5Ala-F (5′-GCT GCC GCA GCA GCC GTG AGC AAG GGC GAG GAG CTG-3′) plus CFPYFP-FP-R (5′-ACT AAT GGG AAA CTT GTA CAG CTC GTC CAT GCC G-3′), and a downstream proviral DNA fragment containing the 5′-DNA fragment of RT and SmaI site from pHIV-$1_{NLSma}$ (17), which had been created to have a SmaI site by changing two nucleotides (2590 and 2593) of pHIV-$1_{NL4-3}$ with a primer pair: FRT-F (5′-TTT CCC ATT AGT CCT ATT GAG ACT GTA-3′) plus NL4-3-RT263-R (5′-CCA GAA ATC TTG AGT TCT CTT ATT-3′). A linker consisting of five alanines was inserted between protease and fluorescent protein. The phenylalanine-proline site that HIV-1 protease cleaves was also introduced between the fluorescent protein and RT. Thus obtained three DNA fragments were subsequently joined by using the PMR reaction performed under the standard condition for ExTaq polymerase (Takara Bio Inc., Otsu, Japan) with 10 pmol of Apa-PRO-F (5′-TTG CAG GGC CCC TAG GAA AAA GG-3′) and NL4-3-RT263-R (5′-CCA GAA ATC TTG AGT TCT CTT ATT-3′) and the three DNA fragments (100 ng each) in a 20-μl reaction solution. Thermal cycling was carried out as follows: 94 °C for 3 min, followed by 35 cycles of 94 °C for 50 s, 53 °C for 50 s, and 72 °C for 2 min, and finally by 72 °C for 15 min. The amplified PCR products were cloned into pCR-XL-TOPO vector according to the manufacturer's instructions (Gateway Cloning System, Invitrogen). PCR products were generated with pCR-XL-TOPO vector as templates, followed by digestion by both ApaI and SmaI, and the ApaI-SmaI fragment was introduced into pHIV-$1_{NLSma}$ (17), generating pHIV-$PR_{WT}^{CFP}$ and pHIV-$PR_{WT}^{YFP}$, respectively.

*Analysis of Inter- and Intra-molecule Interactions of Protease Subunits*—Analysis of inter- and intra-molecule interactions of protease subunits was conducted by employing the crystal structure of DRV with HIV-1 protease (PDB ID: 2IEN). Hydrogens were added and minimized using the OPLS2005 force field with constraints on heavy atom positions. The calculation was performed using MacroModel 9.1 from Schrödinger, LLC. Hydrogen bonds were assigned when the following distance and angle cut-off was satisfied: 3.0 Å for H-A distance; D-H-A angle >90°; and H-A-B angle >60° where H is the hydrogen, A is the acceptor, D is the donor, and B is a neighbor atom bonded to the acceptor. The representative distance between the termini of two monomers was determined by analyzing the protease-DRV crystal structure (PDB ID: 2IEN). The distance between the α carbons at the N termini and C termini is around 0.5 nm, whereas the distance between the α carbons of the N termini ends of two monomers is around 1.8 nm.

*FRET Procedure*—COS7 cells plated on EZ view cover-glass bottom culture plate (Iwaki, Tokyo) were transfected with the indicated plasmid constructs using Lipofectamine 2000 (Invitrogen) according to manufacturer's instructions in the presence of various concentrations of each compound, cultured for 72 h, and analyzed under Fluoview FV500 confocal laser scanning microscope (Olympus Optical Corp., Tokyo) at room temperature. When the effect of each compound was analyzed

by FRET, test compounds were added to the culture medium simultaneously with plasmid transfection.

The results of FRET were determined by quenching of CFP (donor) fluorescence and an increase in YFP (acceptor) fluorescence (sensitized emission), because part of the energy of CFP is transferred to YFP instead of being emitted. This phenomenon can be measured by bleaching YFP, which should result in an increase in CFP fluorescence. This technique, also known as acceptor photobleaching, is a well established method of determining the occurrence of FRET (18–21). Dequenching of the donor CFP by selective photobleaching of the acceptor YFP was performed by first obtaining YFP and CFP images at the same focal plane, followed by illuminating for 3 min the same image at a wavelength of 488 nm with a laser power set at the maximum intensity to bleach YFP and re-capturing the same CFP and YFP images. The changes in the CFP and YFP fluorescence intensity in the images of selected regions were examined and quantified using Olympus FV500 Image software system (Olympus Optical Corp.). Background values were obtained from the regions where no cells were present and were subtracted from the values for the cells examined in all calculations. For each chimeric protein, the data were obtained from at least three independent experiments. Digitized image data obtained from the experiment were prepared for presentation using Photoshop 6.0 (Adobe Systems, Mountain View, CA). Ratios of intensities of CFP fluorescence after photobleaching to CFP fluorescence prior to photobleaching ($CFP^{A/B}$ ratios) were determined. It is well established that the $CFP^{A/B}$ ratios of >1.0 indicate that association of CFP- and YFP-tagged proteins occurred, and it was interpreted that the dimerization of protease subunits occurred. When the $CFP^{A/B}$ ratios were <1, it indicated that the association of the two subunits did not occur, and it was interpreted that protease dimerization was inhibited.

*Non-peptidyl Small Molecule Compounds*—Seven non-peptidyl small molecule compounds were synthesized in a convergent manner by coupling an optically active P2 ligand and an (*R*)-hydroxyethylamino sulfonamide isostere (22). Synthetic methods for TMC126 and DRV have been previously described (22, 23). Detailed synthetic methods for the other four compounds will be described elsewhere. TPV was obtained through the AIDS Research and Reference Reagent Program, Division of AIDS, NIAID, National Institutes of Health.

*Dual Luciferase Assay*—Dual luciferase assay was established using the CheckMate™ Mammalian Two-Hybrid System (Promega Corp., Madison, WI). Briefly, BamHI/KpnI fragments from pCR-XL-TOPO vector containing the HIV-1 protease ($PR_{WT}$)-encoding gene excised from pHIV-$1_{NL4-3}$ was inserted into the pACT vector and pBIND vector that had been digested with BamHI and KpnI, generating pACT-$PR_{wt}$ and pBIND-$PR_{wt}$, which produced an in-frame fusion of wild-type HIV-1 protease downstream of the VP16 activation domain and GAL4 DNA-binding domain, respectively. COS7 cells were co-transfected with pACT-$PR_{wt}$, pBIND-$PR_{wt}$, and pG5*luc* in the absence or presence of 0.1 or 1.0 μM DRV in white 96-well flat bottom plates (Corning, NY), cultured for 48 h, and the intensity of firefly luminescence (Fluc) and *Renilla* luminescence (Rluc) was measured with TR717 microplate luminometer (Applied Biosystems) according to the manufacturer's instructions. DRV was added to the culture medium simultaneously with plasmids to be used. Fluc/Rluc intensity ratios were determined with co-transfection of pACT-$PR_{wt}$, pBIND-$PR_{wt}$, and pG5*luc* in the absence of DRV, serving as maximal values. Fluc/Rluc intensity ratios determined with co-transfection of a pACT vector, a pBIND vector, and pG5*luc* served as minimal (background) values. Relative response ratios (RRR) were determined using the following formula: RRR = [(experimental Fluc/Rluc) − (negative control Fluc/Rluc)]/[(positive control Fluc/Rluc) − (negative control Fluc/Rluc)].

*Drug Susceptibility Assay*—The susceptibility of HIV-$1_{LAI}$ to various drugs and their cytotoxicity were determined using the 3-(4,5-dimethylthiazol-2-yl)-2,5-diphenyltetrazolium bromide assay as previously described (24). Briefly, MT-2 cells ($2 \times 10^4$/ml) were exposed to 100 $TCID_{50}$s of HIV-$1_{LAI}$ in the presence or absence of various concentrations of drugs in 96-well microculture plates and cultured at 37 °C for 7 days. After 100 μl of the medium was removed from each well, 3-(4,5-dimetylthiazol-2-yl)-2,5-diphenyltetrazolium bromide solution (10 μl, 7.5 mg/ml in phosphate-buffered saline) was added to each well, followed by incubation at 37 °C for 4 h. After incubation, 100 μl of acidified isopropanol containing 4% (v/v) Triton X-100 was added to each well, to dissolve the formazan crystals, and the optical density was measured in a kinetic microplate reader ($V_{max}$, Molecular Devices, Sunnyvale, CA). All assays were performed in duplicate or triplicate. In some experiments, MT-2 cells were chosen as target cells in the 3-(4,5-dimethylthiazol-2-yl)-2,5-diphenyltetrazolium bromide assay, because these cells undergo greater HIV-1-elicited cytopathic effects than MT-4 cells. AQ: F

*Enzyme Kinetics*—The chromogenic substrate Lys-Ala-Arg-Val-Nle-pnitroPhe-Glu-Ala-Nle-amide (Sigma) was used to determine the kinetic parameters (25, 26). Wild-type PR, at final concentrations of 160–190 nM, was added to varying concentrations of substrate (100–400 μM) maintained in 50 mM sodium acetate (pH 5.0), 0.1 M NaCl, 1 mM EDTA, and assayed by monitoring the decrease in absorbance at 310 nm using a Varian Cary 100Bio UV-visible spectrophotometer. The $k_{cat}$ and $K_m$ values were obtained employing standard data fitting techniques for a reaction obeying Michaelis-Menten kinetics. The data curves were fitted using SigmaPlot 8.0.2 (SPSS Inc., Chicago, IL). The active enzyme concentrations were calculated from the intercept of the linear fit to the $IC_{50}$ *versus* [S] plots with the $IC_{50}$ axis. The $K_i$ values were obtained from the $IC_{50}$ values estimated from an inhibitor dose-response curve with the spectroscopic assay using the equation $K_i = (IC_{50} - [E]/2)/(1 + [S]/K_m)$, where [*E*] and [S] are the PR and substrate concentrations, respectively (27). The $K_i$ values were measured at four to five substrate concentrations. The measurement was repeated at least three times to produce the average values. AQ: G AQ: H

*Assay for Effects of Darunavir on Dimerized Mature Protease*—To examine whether a representative dimerization inhibitor, DRV, could dissociate mature protease that had already been dimerized, COS7 cells were co-transfected with a pair of plas-

## Potent HIV-1 Inhibition and Protease Dimerization Inhibition

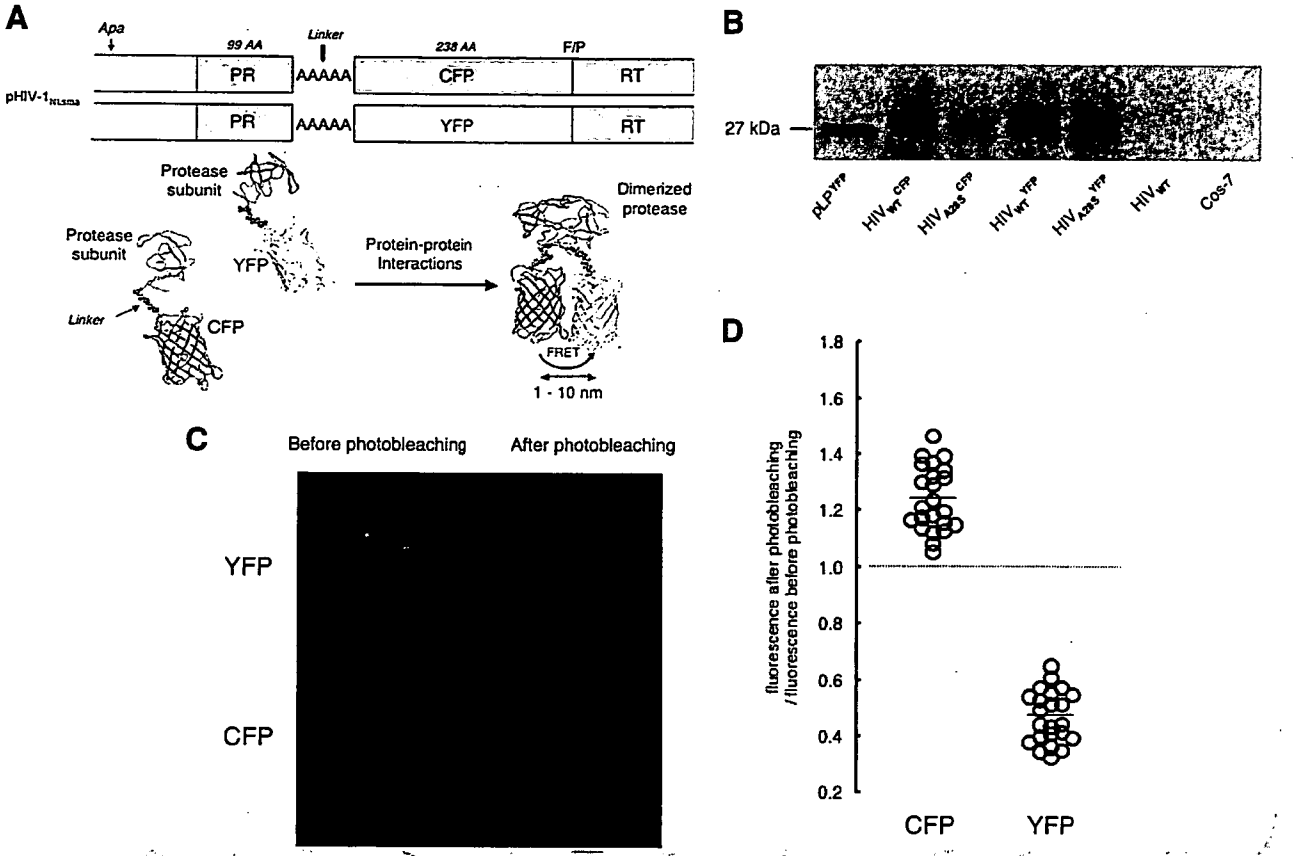


AQ: P FIGURE 1. **FRET-based HIV-1 expression system.** *A*, generation of FRET-based HIV-1 expression system. Various plasmids encoding full-length molecular infectious HIV-1 (HIV-$1_{NL4-3}$) clones producing CFP- or YFP-tagged protease using the PCR-mediated recombination method were prepared. A linker consisting of five alanines was inserted between protease and fluorescent protein. A phenylalanine-proline site (*F/P*) that HIV-1 protease cleaves was also introduced between the fluorescent protein and RT. Shown are structural representations of protease monomers and dimer in association with the linker atoms and fluorescent proteins. FRET occurs only when the fluorescent proteins are 1–10 nm apart. *B*, expression of CFP- and YFP-tagged wild-type HIV-1 protease. To confirm the presence of HIV-1 protease tagged to fluorescent protein in COS7 cells transfected with a plasmid encoding $HIV_{WT}^{CFP}$, $HIV_{A28S}^{CFP}$, $HIV_{WT}^{YFP}$, or $HIV_{A28S}^{YFP}$, Western blot analysis was performed using lysates of pelleted virions. The CFP- and YFP-tagged proteases were visualized by SuperSignal WestPico Chemiluminescent Substrates using polyclonal anti-GFP antiserum and ECL anti-rabbit IgG peroxidase-linked species-specific whole antibody. $pLP^{YFP}$ denotes the lysates of cells transfected with a plasmid encoding only YFP. The lysates of COS7 cells transfected with a plasmid encoding $HIV_{WT}$, and those of untreated COS7 cells serve as controls. *C*, fluorescence images of co-transfected cells prior to and after acceptor photobleaching. COS7 cells plated on EZ view cover-glass bottom culture plate were transfected with two plasmids, $pPR_{WT}^{CFP}$ and $pPR_{WT}^{YFP}$, using Lipofectamine, cultured for 72 h, and analyzed under a Fluoview FV500 confocal laser scanning microscope. Both $PR_{WT}^{CFP}$ and $PR_{WT}^{YFP}$ proteins were visualized prior to photobleaching. Note that photobleaching of the cells dramatically reduced YFP fluorescence with a $YFP^{A/B}$ ratio of 0.17 and increased CFP emission with a $CFP^{A/B}$ ratio of 1.38, signifying the dimerization of both YFP- and CFP-tagged protease subunits. *D*, ratios of the emission intensities before and after photobleaching. Fluorescence intensities of each cell transfected with two plasmids, $pPR_{WT}^{CFP}$ and $pPR_{WT}^{YFP}$, were measured before and after photobleaching, and ratios of the emission intensities before and after photobleaching ($CFP^{A/B}$ ratios) were determined, and plotted. The $CFP^{A/B}$ ratio values were 1.24 ± 0.11 ($n$ = 23), whereas the $YFP^{A/B}$ ratio values were 0.47 ± 0.09 ($n$ = 23). The mean of these ratios are shown as *bars*.

mids encoding HIV-$PR_{WT}^{CFP}$ and HIV-$PR_{WT}^{YFP}$ and exposed to a protein synthesis inhibitor cycloheximide (50 μg/ml, Sigma) at 24, 48, 72, and 96 h of culture following transfection. The cells were then exposed to DRV (1 μM) on day 5 of culture, and the values of the $CFP^{A/B}$ ratio were determined at various time points. When the $CFP^{A/B}$ ratios determined were >1.0, it was determined that HIV-1 protease had been generated and dimerization had occurred. The production of HIV-1 was monitored every 24 h following transfection by determining levels of p24 Gag protein produced into culture medium as previously described (24).

## RESULTS

*Generation of FRET-based HIV-1 Expression Assay*—The basic concepts of the intermolecular FRET-based HIV-1-expression assay (FRET-HIV-1 assay) are shown in Fig. 1. Within a plasmid (pHIV-$1_{NL4-3}$), which encodes a full-length molecular infectious HIV-1 clone, the gene encoding a cyan fluorescent donor protein (CFP) was attached to the downstream end (C terminus) of the gene encoding an HIV-1 protease subunit through the flexible linker added (five alanines), generating pHIV-$1_{NL4-3/CFP}$ (Fig. 1*A*). Within the other plasmid (pHIV-$1_{NL4-3}$), the gene encoding a yellow fluorescent acceptor protein (YFP) was attached to the downstream end of protease-encoding gene in the same manner, generating pHIV-$1_{NL4-3/YFP}$. Both CFP and YFP were designed to have phenylalanine and proline in the connection with reverse transcriptase so that the protease is cleaved from reverse transcriptase when two subunits dimerize and the dimerized protease acquires enzymatic activity. Fig. 1*B* illustrates that HIV-1 virions generated in F1

COS7 cells transfected with pHIV-$1_{NL4-3/CFP}$ contained CFP-tagged protease and those in COS7 cells transfected with pHIV-$1_{NL4-3/YFP}$ contained YFP-tagged protease as examined in Western blotting. The HIV-1 virions produced were capable of infecting $CD4^+$ MT-4 cells when the cells were exposed to the supernatant of the transfected COS7 cells (data not shown), indicating that the expressed tagged protease was enzymatically and virologically functional. In the cytoplasm of COS7 cells co-transfected with pHIV-$1_{NL4-3/CFP}$ and pHIV-$1_{NL4-3/YFP}$, a CFP-tagged protease subunit interacts and dimerizes with a YFP-tagged protease subunit, and CFP and YFP get close because the termini are separated by only 0.5 to 1.8 nm in the dimeric form of protease (note: the representative distance was determined by analyzing the protease-DRV crystal structure (PDB ID: 2IEN)). A focused laser beam excitation of CFP (triggered by helium-cadmium laser) results in rapid energy transfer to YFP, and most of the fluorescence photons are emitted by YFP (28). If the dimerization is blocked, the average distance between CFP and YFP become larger, the energy transfer rate is decreased, and the fraction of photons emitted by YFP is lowered.

To help us interpret the energy transfer efficiency quantitatively, we used the acceptor photobleaching technique, in which the change in CFP emission quenching is measured by comparing the value before and after selectively photobleaching YFP, which prevents problems associated with variable expression levels. In this acceptor photobleaching approach, when FRET occurs, the fluorescence of the CFP donor increases after bleaching the YFP acceptor chromophore, which is recognized as a signature for FRET (18). Thus, the analysis of the change in CFP fluorescence intensity in the same specimen regions, before and after removal of the acceptor, directly relates the energy transfer efficiency to both donor and acceptor fluorescence. Fig. 1*C* illustrates representative images of co-transfected cells prior to and after YFP photobleaching, showing that, following photobleaching, YFP fluorescence of YFP-tagged wild-type protease subunit ($PR_{WT}{}^{YFP}$) was decreased, whereas CFP fluorescence of $PR_{WT}{}^{CFP}$ increased.

To further help us evaluate the energy transfer efficiency, we determined the ratios of cyan fluorescence intensity, determined with a confocal laser scanning microscope, after photobleaching over that before photobleaching (hereafter referred to as $CFP^{A/B}$ ratios). We also determined $YFP^{A/B}$ ratios in the same manner. If the $CFP^{A/B}$ ratios are >1.0, it is thought the energy transfer (or FRET) took place (18), signifying that dimerization of $PR_{WT}{}^{CFP}$ and $PR_{WT}{}^{YFP}$ subunits occurred. Fig. 1*D* shows that in the co-transfected COS7 cells ($n$ = 23), the $CFP^{A/B}$ ratios were all >1.0 ($CFP^{A/B}$ ratios, 1.24 ± 0.11; $YFP^{A/B}$ ratios, 0.47 ± 0.09), demonstrating that dimerization of protease subunits occurred.

*Changes in Fluorescence Emission with Amino Acid Substitutions in Protease*—First, it was determined whether the above-described FRET-HIV-1 assay could be used to detect the disruption of HIV-1 protease dimerization. Five amino acids at the N terminus and those at the C terminus have been shown to be critical for protease dimerization (29). As shown in Fig. 2*A*, two protease monomer subunits are connected by four antiparallel β-sheets involving the N and C termini of both subunits. It is of note that mature dimerized protease has as many as 12 hydrogen bonds in this N- and C-terminal region. Thus, we introduced a Pro-1 to Ala substitution (P1A), Q2A, I3A, T4A, L5A, T96A, L97A, N98A, or F99A substitution into the replication-competent HIV-$1_{NL4-3}$ and found that I3A, L5A, T96A, L97A, and F99A disrupted protease dimerization, although other substitutions did not disrupt the dimerization.

Several amino acid substitutions outside the N and C termini have also been known to play a role in HIV-1 protease dimerization. Ishima and Louis and their colleagues have demonstrated that the introduction of T26A, D29N, D29A, or R87K to HIV-1 protease disrupts the dimer interface contacts and destabilizes protease dimer, causing the inhibition of protease dimerization (30–32). Fig. 2 (*B* and *C*) shows the locations of intermolecular hydrogen bonds formed by such amino acids between two monomer subunits. The hydrogen bond interactions between two subunits occur between Asp-29 and Arg-8′, Arg-87 and Leu-5′, Leu-24 and Thr-26′, and Thr-26 and Thr-26′. There are also intra-molecular hydrogen bond interactions between Asp-29 and Arg-87 as shown in Fig. 2 (*B–D*). Thus, mutations in those amino acids were introduced into HIV-$PR_{WT}{}^{CFP}$ and HIV-$PR_{WT}{}^{YFP}$, generating HIV-$PR_{T26A}{}^{CFP}$, HIV-$PR_{T26A}{}^{YFP}$, HIV-$PR_{D29N}{}^{CFP}$, HIV-$PR_{D29N}{}^{YFP}$, HIV-$PR_{D29A}{}^{CFP}$, HIV-$PR_{D29A}{}^{YFP}$, HIV-$PR_{R87K}{}^{CFP}$, and HIV-$PR_{R87K}{}^{YFP}$. Co-transfection of COS7 cells with a pair of CFP- and YFP-tagged protease-carrying HIV-1-encoding plasmids demonstrated that these four amino acid substitutions disrupted protease dimerization (the average $CFP^{A/B}$ ratios were all <1.0; Fig. 2*E*). Substitutions of two amino acids adjacent to Asp-29 were also introduced, generating HIV-$PR_{A28S}{}^{CFP}$, HIV-$PR_{A28S}{}^{YFP}$, HIV-$PR_{D30N}{}^{CFP}$, and HIV-$PR_{D30N}{}^{YFP}$. Both A28S and D30N are known primary amino acid substitutions, conferring resistance to TMC-126 and nelfinavir on HIV-1, respectively (33, 34). The fact that A28S- or D30N-containing HIV-1 is infectious and replication-competent indicates that these two amino acid substitutions would not disrupt protease dimerization. HIV-1 virions generated in COS7 cells transfected with HIV-$PR_{A28S}{}^{CFP}$ and HIV-$PR_{A28S}{}^{YFP}$ were confirmed to contain CFP-tagged protease and YFP-tagged protease in Western blotting, respectively (Fig. 1*B*). As expected, neither substitution disrupted the dimerization as examined in the FRET-HIV-1 assay (Fig. 2*E*). Another mutation D25A, which is adjacent to Asp-26 and is known to abrogate replicative activity of HIV-1 (35), failed to disrupt protease dimerization, indicating that the inability of D25A mutation-carrying HIV-1 to replicate is not due to dimerization disruption, but due to the loss of proteolytic activity of dimerized HIV-1 protease. Analysis of these data indicated that the FRET-HIV-1 assay system is a reliable tool to evaluate agents for their potential to inhibit protease dimerization.

*Inhibition of Protease Dimerization by Non-peptidyl and Peptidyl Compounds*—After establishing the validity of the FRET-HIV-1 assay to detect protease dimerization inhibition, we evaluated various newly generated non-peptidyl small molecule agents, including the currently available anti-HIV-1 drugs for their ability to inhibit protease dimerization in a blind manner, where agents examined were identified only under code in conducting the FRET-HIV-1 assay. Six different non-peptidyl small

## *Potent HIV-1 Inhibition and Protease Dimerization Inhibition*

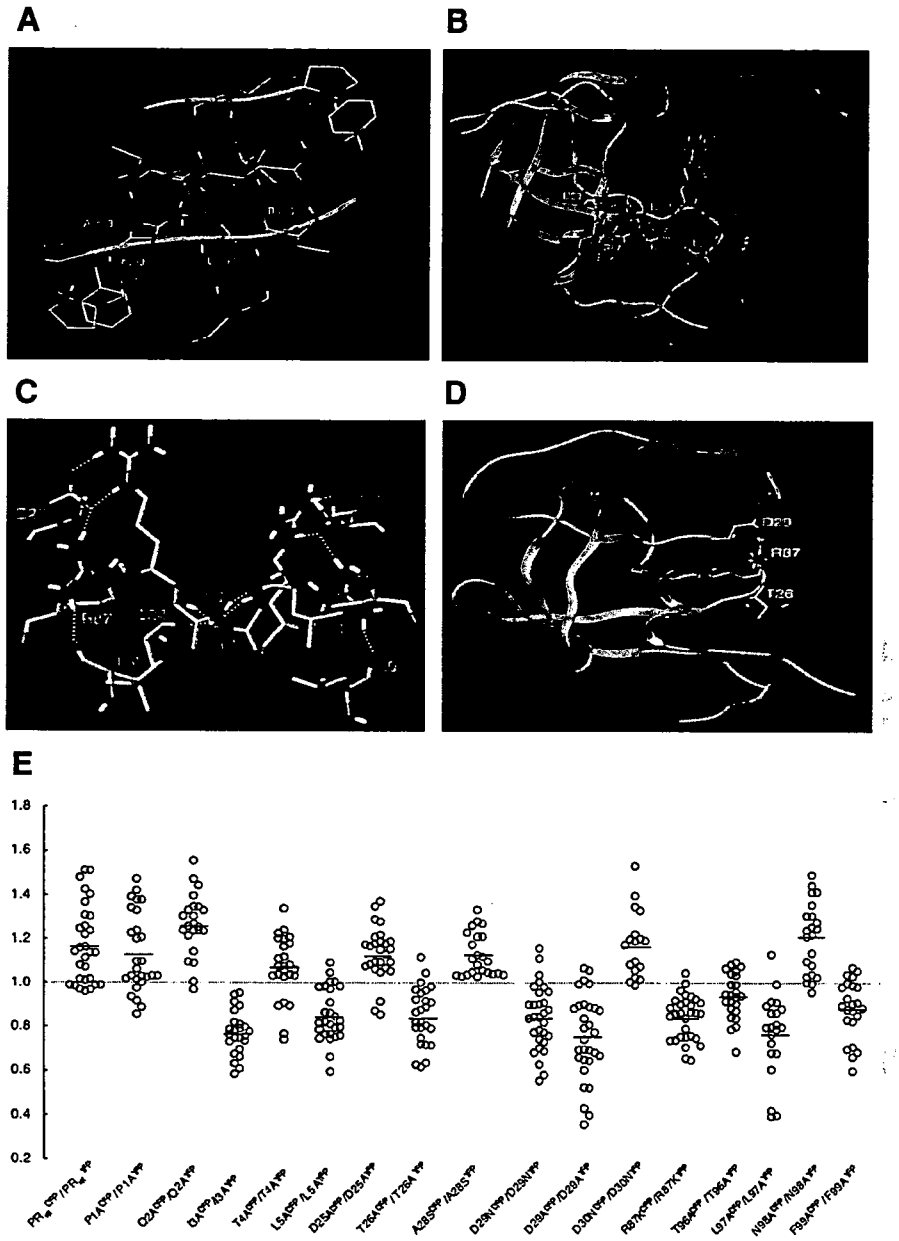


FIGURE 2. **Critical amino acid residues for protease dimerization.** *A*, four antiparallel β-sheets involving the N and C termini of both monomer subunits. Two HIV-1 protease monomer subunits are connected by four antiparallel β-sheets involving the N and C termini of both monomer subunits. It is of note that mature dimerized protease has as many as 12 hydrogen bonds in this N- and C-terminal region, and these interactions seem to be critical for dimer formation. A monomer subunit is shown by the *green ribbon*, and the other monomer subunit is shown by the *red ribbon*. A molecule disrupting these inter-protease hydrogen bond contacts can also disrupt their dimerization. *B* and *C*, intermolecular hydrogen bonds between two HIV-1 protease monomer subunits. The figure shows the intermolecular hydrogen bonds between two protease monomer subunits. The hydrogen bond interactions between protease monomer A (shown as *green ribbon*) and monomer B (shown in *red ribbon*) are Asp-29 to Arg-8', Arg-87 to Leu-5', Leu-24 to Thr-26', and Thr-26 to Thr-26'. The corresponding amino acids of monomer B also form hydrogen bonds with monomer A (*i.e.* Asp-29' to Arg-8, etc.). Intra-molecular hydrogen bond interaction between Asp-29 and Arg-87 is shown by *white dotted lines*. The residues forming critical intermolecular contacts between two monomer subunits are shown by atom color types (C, *gray*; N, *blue*; O, *red*; and H, *white*). Only polar hydrogens are shown. The residues of chain A are labeled *green*, and those of chain B are labeled *red*. This provides a structural explanation to the FRET experimental data, which show that mutations Leu-5, Asp-29, Asp-26, and Arg-87 prevent formation of a protease dimer. *D*, potential binding sites of the small molecule dimerization inhibitors. The figure shows one of the potential binding sites of the dimerization inhibitors. Asp-29, Arg-87, and Thr-26 are spatially close enough to form binding interactions with the dimerization inhibitor and prevent the other protease monomer from interacting with these residues. *E*, changes in emission intensity ratios upon amino acid substitution. COS7 cells were co-transfected with a pair of HIV-$PR^{CFP}$ and HIV-$PR^{YFP}$ carrying wild-type protease or protease with one amino acid substitution, and $CFP^{A/B}$ ratios were determined. The $CFP^{A/B}$ ratio value for $PR_{WT}{}^{CFP}/PR_{WT}{}^{YFP}$ was 1.17 ± 0.18 (mean ± 1 S.D.); $PR_{P1A}{}^{CFP}/PR_{P1A}{}^{YFP}$, 1.13 ± 0.18; $PR_{Q2A}{}^{CFP}/PR_{Q2A}{}^{YFP}$, 1.26 ± 0.14; $PR_{I3A}{}^{CFP}/PR_{I3A}{}^{YFP}$, 0.77 ± 0.10; $PR_{T4A}{}^{CFP}/PR_{T4A}{}^{YFP}$, 1.07 ± 0.14; $PR_{L5A}{}^{CFP}/PR_{L5A}{}^{YFP}$, 0.85 ± 0.12; $PR_{D25A}{}^{CFP}/PR_{D25A}{}^{YFP}$, 1.13 ± 0.12; $PR_{T26A}{}^{CFP}/PR_{T26A}{}^{YFP}$, 0.84 ± 0.13; $PRA_{285}{}^{CFP}/PR_{A285}{}^{YFP}$, 1.13 ± 0.10; $PR_{D29N}{}^{CFP}/PR_{D29N}{}^{YFP}$, 0.84 ± 0.15; $PR_{D29A}{}^{CFP}/PR_{D29A}{}^{YFP}$, 0.76 ± 0.19; $PR_{D30N}{}^{CFP}/PR_{D30N}{}^{YFP}$, 1.17 ± 0.15; $PR_{R87K}{}^{CFP}/PR_{R87K}{}^{YFP}$, 0.84 ± 0.10; $PR_{T96A}{}^{CFP}/PR_{T96A}{}^{YFP}$, 0.94 ± 0.10; $PRL_{97A}{}^{CFP}/PR_{L97A}{}^{YFP}$, 0.77 ± 0.19; $PR_{N98A}{}^{CFP}/PR_{N98A}{}^{YFP}$, 1.21 ± 0.16; and $PR_{F99A}{}^{CFP}/PR_{F99A}{}^{YFP}$, 0.88 ± 0.13. All the experiments were conducted in a blind fashion. The $CFP^{A/B}$ ratio that is >1 signifies a protease dimer, whereas a ratio that is <1 signifies disruption of protease dimerization. Note that the residue (such as Ile-3 or Asp-29) whose mutation resulted in disruption of dimerization had an inter-molecular hydrogen bond contact with the other protease monomer as shown in *A*–*C*. The mean value of the ratios is shown as *bars*.

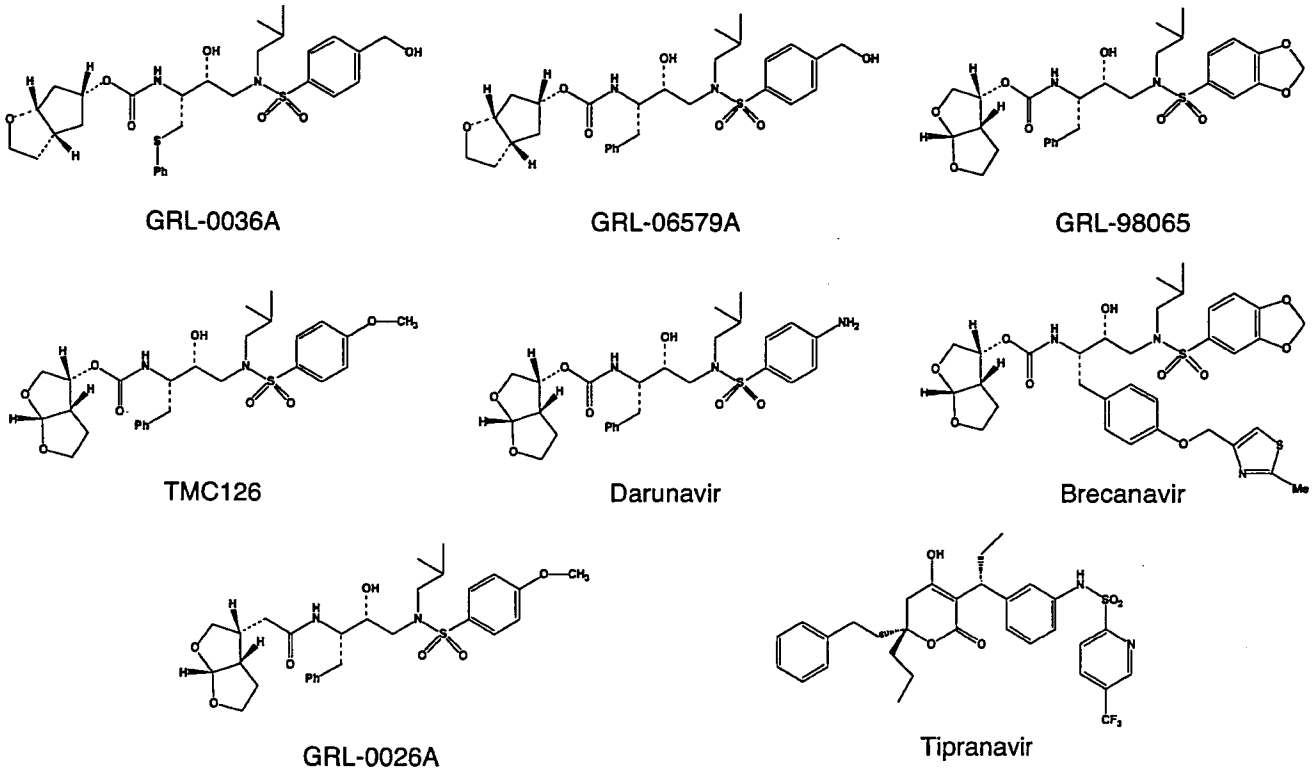


FIGURE 3. **Structures of dimerization inhibitors identified.** Structures of eight dimerization inhibitors are shown. The $IC_{50}$ values for activity against HIV-1 in acute HIV-1 infection assays are shown in Table 1.

molecule agents (GRL-0036A, GRL-06579A (26), TMC126 (33), GRL-98065 (36), DRV (24), and brecanavir (BCV) (37); $M_r$, ranging from 547 to 704 (Fig. 3)) were found to disrupt protease dimerization at concentration of 1 μM in the assay (Fig. 4*A*). All of these agents had potent inhibitory activity against HIV-1 protease with $K_i$ values of 29, 3.5, 10, 14, 16, and 6.8 pM, respectively, as examined in the assay previously described (25, 26), and were highly potent against HIV-$1_{LAI}$ in acute HIV-1 infection assays using target $CD4^+$ MT-2 cells (24) with $IC_{50}$ values of 0.0002–0.005 μM (Table 1). In addition to small molecule agents, we examined various peptides in the FRET-HIV-1 assay. A 27-amino acid peptide containing the dimer interface sequences amino acids 1–5 and amino acids 95–99 (P27: PQITLRKKRRQRRRPPQVSFNFATLNF), which blocks HIV-1 infectivity and replication (14), also inhibited protease dimerization as examined in the FRET-HIV-1 expression assay. Another peptide P9 (RKKRRQRRRPPQVSFNF) that lacks the dimer interface sequences and is not active against HIV-1 (14) failed to inhibit protease dimerization in the FRET-HIV-1 assay. These data again corroborated the utility of the assay to evaluate protease dimerization.

To test the robustness and reproducibility of the FRET-HIV-1 assay data, we determined the $CFP^{A/B}$ ratios in a total of 143 COS7 cells transfected with $pPR_{WT}{}^{CFP}$ and $pPR_{WT}{}^{YFP}$ plasmids and cultured in the presence or absence of 1 μM DRV for 3 days on 11 different occasions. In the presence of DRV, only 7 (4.9%) of 143 cells had the ratios of slightly more than 1.0, whereas all the rest (95.1%) had values of <1.0 ($n$ = 143; average of 0.73 ± 0.22) (Fig. 4*B*). The $CFP^{A/B}$ ratios determined in the absence of DRV were mostly >1.0 ($n$ = 172, average of 1.21 ± 0.17). We next examined whether a dose response in the dimerization inhibition could be seen when the cells were exposed to various concentrations of DRV. As shown in Fig. 4*C*, DRV effectively inhibited protease dimerization at concentrations of 0.1 μM and above, whereas the average $CFP^{A/B}$ ratio was slightly >1.0 at 0.01 μM, and no dimerization inhibition was seen at 0.001 μM. These data show that the inhibition by DRV was roughly dose-responsive up to 0.1 μM. In addition, we examined a TMC126-congener GRL-0026A (Fig. 3) that is substantially less potent than TMC126 against HIV-1 with $IC_{50}$ of 0.48 μM (Table 1), along with TMC126 and BCV for their dose response dimerization inhibition in the FRET-HIV-1 assay and found that the inhibition was similarly dose-responsive (Fig. 4*D*).

*None of the FDA-approved Anti-HIV-1 Drugs Except TPV Blocks Dimerization*—We asked whether other currently approved PIs blocked protease dimerization in the FRET-HIV-1 assay. None of the seven PIs (saquinavir, nelfinavir, amprenavir, indinavir, ritonavir, lopinavir, and atazanavir) inhibited protease dimerization at 1 μM concentration, whereas the control DRV clearly inhibited the dimerization as shown in Fig. 4*E*. Considering that DRV is generally more potent against HIV-1 *in vitro* than most currently existing PIs (24), four PIs (saquinavir, amprenavir, nelfinavir, and atazanavir) were examined in the FRET-HIV-1 assay at a higher concentration, 10 μM, however, none of these four PIs inhibited protease dimerization (Fig. 4*F*). Interestingly, TPV, which has been shown to provide more favorable virological and immunological responses in patients who have received extensive previous antiretroviral

## *Potent HIV-1 Inhibition and Protease Dimerization Inhibition*

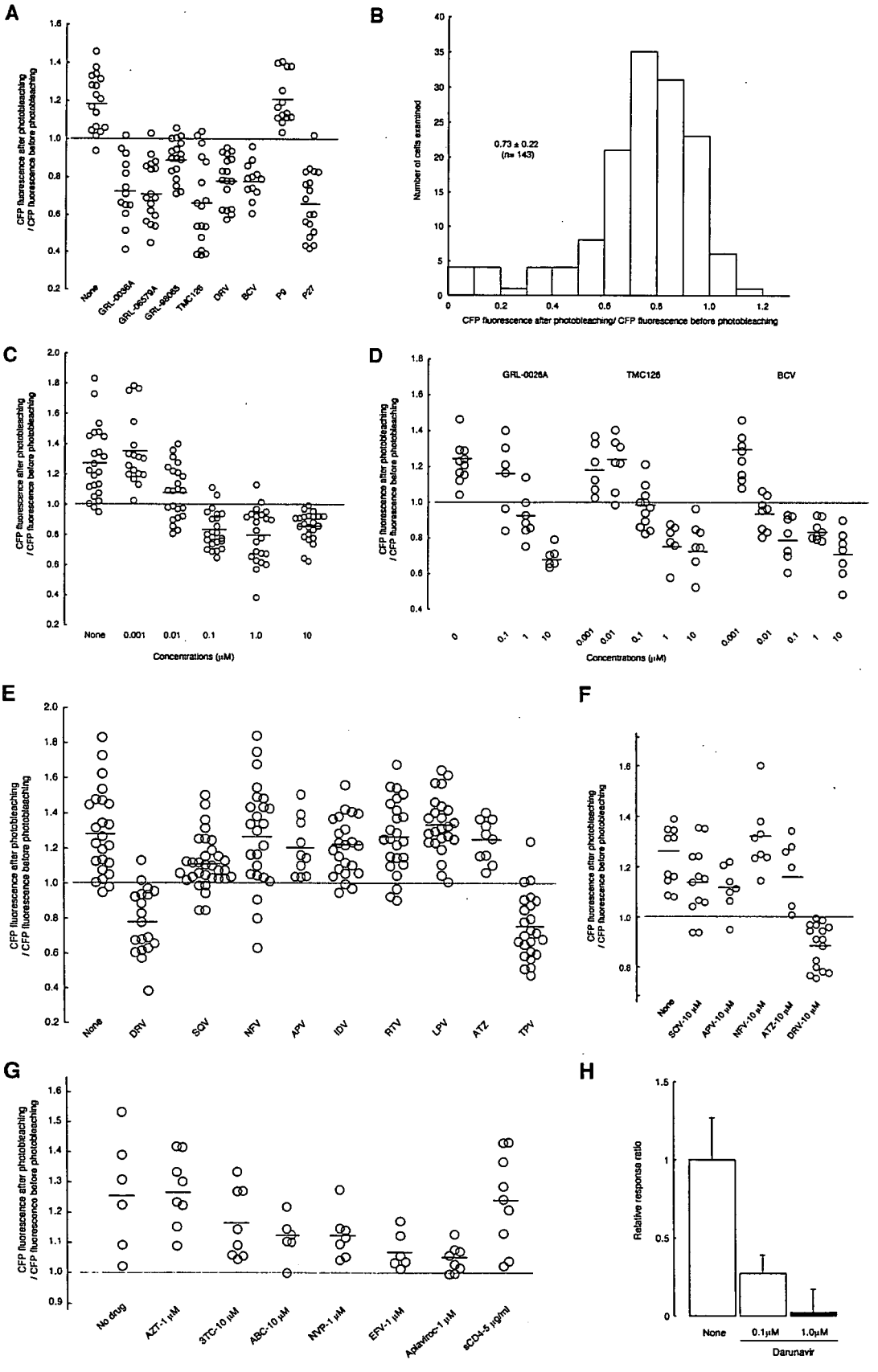

**TABLE 1**

**Antiviral activity and enzyme inhibition of protease dimerization inhibitors**

MT-2 cells ($2 \times 10^5$) were exposed to 100 $TCID_{50}$ values of HIV-$1_{LAI}$ and cultured in the presence of various concentrations of each drug, and the $IC_{50}$ values were determined using the 3-(4,5-dimethylthiazol-2-yl)-2,5-diphenyltetrazolium bromide assay. All assays were conducted in duplicate, and the data shown represent mean values (±1 S.D.) derived from the results of three independent experiments. The chromogenic substrate Lys-Ala-Arg-Val-Nle-pnitroPhe-Glu-Ala-Nle-amide was used to determine the kinetic parameters. The $K_i$ values were obtained from the $IC_{50}$ values estimated from an inhibitor dose-response curve with the spectroscopic assay using the equation $K_i = (IC_{50} - [E]/2)/(1 + [S]/K_m)$, where $[E]$ and $[S]$ are the PR and substrate concentrations, respectively. The $K_i$ values were measured at four to five substrate concentrations. The measurement was repeated at least three times to produce the average values.

| Drug | $IC_{50}$ | $K_i$ |
|---|---|---|
| | μM | pM |
| GRL-0036A | 0.005 ± 0.002 | 29 |
| GRL-06579A | 0.0014 ± 0.0008 | 3.5 |
| GRL-98065 | 0.0004 ± 0.0001 | 14 |
| TMC126 | 0.0003 ± 0.0001 | 10 |
| DRV | 0.0034 ± 0.0005 | 16 |
| BCV | 0.0002 ± 0.0001 | 6.8 |
| GRL-0026A | 0.48 ± 0.04 | ND[a] |
| TPV | 0.10 ± 0.04 | ND |

[a] ND, not determined.

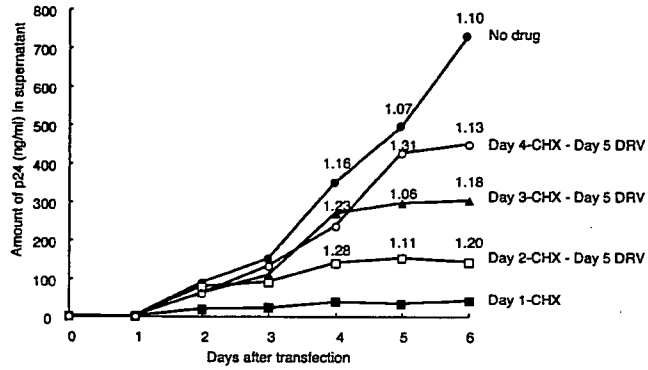


FIGURE 5. **Darunavir does not dissociate once-dimerized protease in cells producing infectious HIV-1 virions.** COS7 cells were co-transfected with two plasmids, $pPR_{WT}^{CFP}$ and $pPR_{WT}^{YFP}$, exposed to CHX (50 μg/ml) in 24, 48, 72, and 96 h of culture. The cells were exposed to DRV on day 5 of culture. The production of HIV-1 was monitored every 24 h by determining levels of p24 Gag protein produced into culture medium. The values of the $CFP^{A/B}$ ratio were determined at various time points.

treatment than an optimized background regimen when administered with ritonavir (38), also blocked protease dimerization (Fig. 4*E*).

We also examined various nucleoside and non-nucleoside reverse transcriptase inhibitors (zidovudine, lamivudine, abacavir, nevirapine, and efavirenz) as well as CCR5 inhibitor aplaviroc (39) for dimerization inhibition. However, none of these anti-HIV-1 agents showed inhibition of dimerization even at relatively higher concentrations of 1–10 μM. Soluble CD4 (5 μg/ml) also failed to inhibit protease dimerization (Fig. 4*G*).

*Darunavir Blocks Protease Dimerization as Examined in Dual Luciferase Assay*—We also established a dual luciferase assay using the CheckMate™ Mammalian Two-Hybrid System to examine whether DRV blocked protease dimerization in a different assay system. We generated pACT-$PR_{wt}$, producing $PR_{wt}$, whose N terminus is connected to the herpes simplex virus VP16 activation domain, and pBIND-$PR_{wt}$, producing $PR_{wt}$, whose N terminus is connected to GAL4 DNA-binding domain. In this system, interactions between two different $PR_{wt}$ result in an increase in firefly luciferase expression produced by the pG5*luc* vector. In addition, the pBIND vector expresses *Renilla* luciferase under the control of the SV40 promoter, allowing the user to normalize for the differences in transfection efficiency. Thus, when VP16 and GAL4 closely interact upon protease dimerization, the ratio of the intensity of firefly luminescence (Fluc) over that of *Renilla* luminescence (Rluc) increases, and its decrease indicates the disruption of protease dimerization. As shown in Fig. 4*H*, in the presence of 0.1 and 1 μM of DRV, the relative response ratios significantly decreased, further corroborating that DRV blocks protease dimerization.

*Darunavir Does Not Dissociate Once-dimerized Protease in Cells Producing Infectious HIV-1 Virions*—Finally, an attempt was made to determine if dimerization inhibitors could dissociate mature protease that had already dimerized. COS7 cells were co-transfected with a pair of plasmids encoding HIV-$PR_{WT}^{CFP}$ and HIV-$PR_{WT}^{YFP}$ and exposed to a protein synthesis inhibitor cycloheximide (CHX, 50 μg/ml) at 24, 48, 72, and 96 h of culture. The cells were then exposed to DRV on day 5 of culture, the production of HIV-1 was monitored every 24 h by determining levels of p24 Gag protein produced into culture medium, and the values of the $CFP^{A/B}$ ratio were determined at various time points (Fig. 5). When the cells were treated with CHX on day 1 and throughout the rest of the culture period, only a small amount of p24 Gag protein production was seen but no cells emitting fluorescence were observed. When the

FIGURE 4. **Inhibition of protease dimerization.** *A*, inhibition of protease dimerization by non-peptidyl and peptidyl compounds. COS7 cells were exposed to each of the agents (1 μM of GRL-0036A, GRL-06579A, GRL-98065, TMC126, DRV, and BCV and 10 μM of P9 and P27) and subsequently co-transfected with $pPR_{WT}^{CFP}$ and $pPR_{WT}^{YFP}$. After 72 h, cultured cells were examined in the FRET-HIV-1 assay system using confocal microscopy Fluoview FV500 confocal laser scanning microscope, and $CFP^{A/B}$ ratios were determined and plotted. The mean of these ratios obtained are shown as *bars*. *B*, distribution of the values of $CFP^{A/B}$ ratio in the presence of 1 μM DRV. 143 cells obtained from 11 independent assays were examined, and $CFP^{A/B}$ ratios determined were plotted. All the assays were conducted in a blinded manner. *C*, dose-responsive dimerization inhibition by DRV. COS7 cells were exposed to various concentrations of DRV, co-transfected with $pPR_{WT}^{CFP}$ and $pPR_{WT}^{YFP}$, and A/B ratios were determined. *D*, dose-responsive dimerization inhibition by various non-peptidyl compounds. COS7 cells were exposed to various concentrations of GRL-0026A, TMC126, and BCV, co-transfected with $pPR_{WT}^{CFP}$ and $pPR_{WT}^{YFP}$, and cultured for 72 h. At the end of the culture, $CFP^{A/B}$ ratio values were determined. *E*, failure of seven clinically available protease inhibitors except DRV and TPV to inhibit the dimerization of $PR_{WT}^{CFP}$ and $PR_{WT}^{YFP}$. COS7 cells were co-transfected with $pPR_{WT}^{CFP}$ and $pPR_{WT}^{YFP}$ in the presence of various anti-HIV-1 protease inhibitors at concentration of 1 μM, and A/B ratios were determined. *F*, failure of a high concentration of four clinically available protease inhibitors to inhibit HIV-1 protease dimerization. COS7 cells were co-transfected with $pPR_{WT}^{CFP}$ and $pPR_{WT}^{YFP}$ in the presence of four PIs (saquinavir, amprenavir, nelfinavir, and atazanavir) at a higher concentration of 10 μM, cultured for 72 h, and $CFP^{A/B}$ ratios were determined. Note that all the $CFP^{A/B}$ ratio values were >1.0 except for those of DRV. *G*, various approved anti-HIV-1 agents failed to inhibit HIV-1 protease dimerization. COS7 cells were co-transfected with $pPR_{WT}^{CFP}$ and $pPR_{WT}^{YFP}$ in the presence of various nucleoside and non-nucleoside reverse transcriptase inhibitors (zidovudine, lamivudine, abacavir, nevirapine, and efavirenz), CCR5 inhibitor aplaviroc, and soluble CD4, and A/B ratios were determined. *H*, protease dimerization inhibition by DRV on dual luciferase assay. COS7 cells were co-transfected with pACT-$PR_{wt}$, pBIND-$PR_{wt}$, and pG5*luc* in the presence or absence of 0.1 or 1.0 μM of DRV, cultured for 48 h, and the intensity of firefly luminescence (*Fluc*) and *Renilla* luminescence (*Rluc*) was measured with TR717 microplate luminometer. DRV was added to the culture medium simultaneously with plasmids to be used. Fluc/Rluc intensity ratios were determined with co-transfection of pACT-$PR_{wt}$, pBIND-$PR_{wt}$, and pG5*luc* in the absence of DRV, serving as maximal values.

balt3/zbc-bc/zbc-bc/zbc04007/zbc1091-07z | xppws S=1 | 2/8/07 8:33 | 4/Color Figure(s) F1,2 | ARTNO: M703938200



cells were exposed to CHX on day 2 and beyond, Gag protein production was readily detected by day 2, but no significant increment in the production of p24 Gag protein was seen on those days subsequent to the addition of CHX. When the cells were exposed to CHX on days 3 and 4, greater amounts of Gag protein were seen (Fig. 5). The $CFP^{A/B}$ ratios determined on days 4 and 5 of culture were all >1.0, signifying that HIV-1 protease had been generated and dimerization had occurred. On day 5, DRV (1 $\mu$M) was added to all the cultures described above and the $CFP^{A/B}$ ratios were determined on day 6 of culture. The ratios remained >1.0 in all of the cultured COS7 cells (Fig. 5). These data strongly suggest that DRV does not dissociate mature protease once dimerized within the HIV-1-producing COS7 cells.

## DISCUSSION

In the present study, we developed an intermolecular FRET-based HIV-1-expression assay (FRET-HIV-1 expression assay) that employed cyan and yellow fluorescent protein-tagged HIV-1 protease monomers. Using this assay, we identified a group of non-peptidyl small molecule inhibitors of HIV-1 protease dimerization (molecular weight, 547–704). Dimerization of HIV-1 protease subunits is an essential process for the acquisition of proteolytic activity of HIV-1 protease, which plays a critical role in the replication cycle of HIV-1. Hence, the inhibition of dimerization of HIV-1 protease subunits represents a unique target for potential intervention of HIV-1 replication. The strategy to target protease dimerization as a possible anti-HIV-1 modality has been explored (8, 11–13), and certain compounds have been reported as potential protease dimerization inhibitors. However, no direct evidence of dimerization inhibition by such compounds has been documented. The present report represents the first demonstration that non-peptidic small molecule agents can disrupt protease dimerization.

The structural feature that is in common to the four dimerization inhibitors (TMC126 (33), GRL-98065 (36), DRV (24), and BCV (37)) is that all of these agents contain the structure-based designed privileged cyclic ether-derived non-peptidyl P2 ligand, 3(*R*),3$\alpha$(*S*),6$\alpha$(*R*)-bistetrahydrofuranylurethane (bis-THF) and a sulfonamide isostere (22, 23). GRL-0036A and GRL-06579A (26) have bis-THF-related ligand instead of bis-THF. Crystallographic data of dimerized protease complexed with three dimerization inhibitors (GRL-98065 (36), TMC-126,[3] and DRV (40)) have revealed that bis-THF forms three tight hydrogen bond interactions with Asp-29 and Asp-30, two highly conserved catalytic site amino acids. We also observed that TPV has the ability to disrupt protease dimerization. TPV, which does not possess the bis-THF component, also has interactions with both Asp-29 and Asp-30 through its pyridinesulfonamide group, as shown in crystallographic analysis of a dimerized protease complexed with TPV (41). Thus, the inhibition of protease dimerization is not inherent only to the bis-THF component.

Most of the dimerization inhibitors we examined in this study exerted potent activity against PI-resistant protease in addition to their potent activity to wild-type HIV-1. DRV is potent against $HIV\text{-}1_{NL4\text{-}3}$ variants exposed to and selected for resistance to saquinavir, indinavir, nelfinavir, and ritonavir (24). Crystal structures of HIV-1 protease with a single mutation (D30N, I50V, V82A, I84V, or L90M) complexed with DRV demonstrate that DRV not only binds to the same catalytic active site as it does for wild-type protease but also maintains hydrogen bond interactions with the backbone atoms of Asp-29 and Asp-30 (40, 42). GRL-06579A and GRL-98065 are also potent against multidrug resistant HIV-1 strains, and molecular modeling indicates that for multidrug-resistant clinical isolates, these inhibitors maintain many of the interactions to critical active site residues (26, 36). TPV, which is active against HIV-1 carrying multidrug-resistant protease, also maintains critical hydrogen bond interactions with backbone atoms in the catalytic active site of mutant protease (43).

It is of note that the D30N-carrying HIV-1 variant is infectious and replication-competent (34). Structural studies do not show any hydrogen bond interactions between two monomer proteases mediated through Asp-30, and the FRET-HIV-1 expression assay showed that D30N mutant did not disrupt protease dimerization. This suggests that Asp-30 is not a critical residue for disrupting protease dimerization, and the interaction of these inhibitors with Asp-30 is not linked to the observed dimerization inhibition. However, potential interactions of dimerization inhibitors such as DRV involving Asp-29 could be critical, because D29N and D29A mutations disrupted protease dimer formation (Fig. 2*E*). Our analysis using the FRET-HIV-1 expression assay also revealed that the introduction of T26A and R87K to HIV-1 protease disrupted protease dimerization (the average $CFP^{A/B}$ ratios were all <1.0 (Fig. 2*E*)). If the protease monomer takes a configuration comparable to that in the dimerized protease, it is possible that the hydrogen bonding of the inhibitors with Asp-29, and/or Thr-26 and Arg-87, both of which are in the vicinity of Asp-29 and could be critical for dimerization, could be associated with the disruption of dimerization process through affecting the intermolecular and/or intramolecular hydrogen bond network (Fig. 2, *B–D*). In this regard, Ishima *et al.* (30) have shown that a truncated protease monomer takes a configuration similar to the one in the mature dimerized protease; however, it is unknown whether the untruncated monomer subunit takes a similar mature configuration. Furthermore, it is not known as to what stage of protease maturation (before dimerization) the dimerization inhibitors reported here bind to the monomer subunit in.

Another possible mechanism of the dimerization inhibition by the agents reported here is that they might interact with another dimerization interface formed by an interdigitation of the N- and C-terminal portions of each monomer (residues 1–5 and 95–99 (Fig. 2*A*)). In this regard, when we introduced a Pro-1 to Ala substitution (P1A), Q2A, I3A, T4A, L5A, T96A, L97A, N98A, or F99A into the replication-competent $HIV\text{-}1_{NL4\text{-}3}$, five substitutions (I3A, L5A, T96A, L97A, and F99A) produced the ratios of less than 1.0, strongly suggesting that most of the protease monomer subunit failed to dimerize with each of these five substitutions. These data confirmed the five amino acids at the N terminus and those at the C terminus are

[3] Y. Koh, S. Matsumi, D. Das, M. Amano, D. A. Davis, J. Li, S. Leschenko, A. Baldridge, T. Shioda, R. Yarchoan, A. K. Ghosh, and H. Mitsuya, unpublished observation.

critical for protease dimerization (30–32). There are no polar interactions involving Q2A or T4A, so it is not surprising that these mutations did not affect dimer formation. However, the failure of P1A and N98A to disrupt dimerization does not necessarily indicate that these amino acids are not critical for protease dimerization. It is possible that conversion to a residue other than alanine may disrupt dimerization.

In the present study, DRV failed to dissociate mature protease dimer (Fig. 5). It is of note that mature dimerized protease has as many as 12 hydrogen bonds in the N- and C-terminal regions, which may explain in part why DRV failed to dissociate two subunits of mature protease. These data also suggest that protease dimerization is inhibited before the association of two protease subunits occurs, probably when protease is in the form of nascent Gag-Pol polyprotein. However, the absence of structural data of nascent forms of protease subunit-containing polyprotein makes it difficult to conclusively predict how the dimerization inhibitors inhibit protease dimerization.

It is noteworthy that the D25N substitution, which is known to render HIV-1 protease enzymatically inactive (44), failed to disrupt dimerization (Fig. 2*E*), showing that catalytically inactive subunits are still capable of undergoing dimerization. This observation indicates that the dimerization inhibition is a differing event than the process that confers catalytic activity on two protease monomer subunits.

DRV has a potent activity against a wide spectrum of HIV-1 isolates, including highly multiprotease-inhibitor-resistant HIV-1 variants. The emergence of DRV-resistant HIV-1 seems to be substantially delayed both *in vitro* (45) and clinical settings (46, 47). One can speculate that DRV inhibits protease dimerization, leaving catalytically inert monomers, but if certain monomers escape from DRV and achieve the mature dimer form, DRV again blocks the proteolytic action of mature (wild-type and mutant) protease as a conventional protease inhibitor. This dual anti-HIV-1 function of DRV may explain why DRV is such a highly effective anti-HIV-1 therapeutic and differentiates it from many of the currently available protease inhibitors (46, 47). It is of note that the plasma concentrations of DRV achieved in those receiving DRV and ritonavir remain >2 $\mu$g/ml or ~3.66 $\mu$M (48). These concentrations substantially exceed the concentration of DRV effectively disrupting protease dimerization (0.1 $\mu$M in culture as shown in Fig. 4*C*). Hence, the dimerization inhibition by DRV should be in operation in the clinical settings. Furthermore, DRV could more efficiently disrupt protease dimerization in individuals with HIV-1 infection receiving DRV and ritonavir, because the protease expression levels upon transfection in this study appear to be considerably greater than the protease expression levels *in vivo*, considering that the p24 production levels could be as high as 500–1500 ng/ml by 5 days following transfection of COS7 cells with plasmids used in the FRET-HIV-1 expression assay. The inhibition of HIV-1 protease dimerization by non-peptidyl small molecule agents represents a unique mechanism of HIV-1 intervention, and the dually functional inhibitors reported here might serve as potential candidates as a new class of therapeutic agents for HIV-1 infection and AIDS. The present data should not only help design and examine agents that potentially inhibit HIV-1 protease dimerization but also should give new insights into the process and dynamics of HIV-1 protease dimerization *per se*.

*Acknowledgments—We thank Philip Yin and Kenji Maeda for critical reading of the manuscript, Toshikazu Miyakawa for helpful discussion, and Maki Nakayama for technical assistance.*

REFERENCES

1. Simon, V., and Ho, D. D. (2003) *Nat. Rev. Microbiol.* **1,** 181–190
2. Carr, A. (2003) *Nat. Rev. Drug Discov.* **2,** 624–634
3. Wlodawer, A., Miller, M., Jaskolski, M., Sathyanarayana, B. K., Baldwin, E., Weber, I. T., Selk, L. M., Clawson, L., Schneider, J., and Kent, S. B. (1989) *Science* **245,** 616–621
4. Kohl, N. E., Emini, E. A., Schleif, W. A., Davis, L. J., Heimbach, J. C., Dixon, R. A., Scolnick, E. M., and Sigal, I. S. (1988) *Proc. Natl. Acad. Sci. U. S. A.* **85,** 4686–4690
5. Lapatto, R., Blundell, T., Hemmings, A., Overington, J., Wilderspin, A., Wood, S., Merson, J. R., Whittle, P. J., Danley, D. E., Geoghegan, K. F., *et al.* (1989) *Nature* **342,** 299–302
6. Spinelli, S., Liu, Q. Z., Alzari, P. M., Hirel, P. H., and Poljak, R. J. (1991) *Biochimie (Paris)* **73,** 1391–1396
7. Strisovsky, K., Tessmer, U., Langner, J., Konvalinka, J., and Krausslich, H. G. (2000) *Protein Sci.* **9,** 1631–1641
8. Levy, Y., Caflisch, A., Onuchic, J. N., and Wolynes, P. G. (2004) *J. Mol. Biol.* **340,** 67–79
9. Levy, Y., and Caflisch, A. (2003) *J. Phys. Chem. B* **107,** 3068–3079
10. Todd, M. J., Semo, N., and Freire, E. (1998) *J. Mol. Biol.* **283,** 475–488
11. Bowman, M. J., Byrne, S., and Chmielewski, J. (2005) *Chem. Biol.* **12,** 439–444
12. Frutos, S., Rodriguez-Mias, R. A., Madurga, S., Collinet, B., Reboud-Ravaux, M., Ludevid, D., and Giralt, E. (2007) *Biopolymers* **88,** 164–173
13. Bannwarth, L., Kessler, A., Pethe, S., Collinet, B., Merabet, N., Boggetto, N., Sicsic, S., Reboud-Ravaux, M., and Ongeri, S. (2006) *J. Med. Chem.* **49,** 4657–4664
14. Davis, D. A., Brown, C. A., Singer, K. E., Wang, V., Kaufman, J., Stahl, S. J., Wingfield, P., Maeda, K., Harada, S., Yoshimura, K., Kosalaraksa, P., Mitsuya, H., and Yarchoan, R. (2006) *Antiviral Res.* **72,** 89–99
15. Hoess, R. H., and Abremski, K. (1984) *Proc. Natl. Acad. Sci. U. S. A.* **81,** 1026–1029
16. Fang, G., Weiser, B., Visosky, A., Moran, T., and Burger, H. (1999) *Nat. Med.* **5,** 239–242
17. Gatanaga, H., Suzuki, Y., Tsang, H., Yoshimura, K., Kavlick, M. F., Nagashima, K., Gorelick, R. J., Mardy, S., Tang, C., Summers, M. F., and Mitsuya, H. (2002) *J. Biol. Chem.* **277,** 5952–5961
18. Sekar, R. B., and Periasamy, A. (2003) *J. Cell Biol.* **160,** 629–633
19. Bastiaens, P. I., Majoul, I. V., Verveer, P. J., Soling, H. D., and Jovin, T. M. (1996) *EMBO J.* **15,** 4246–4253
20. Bastiaens, P. I., and Jovin, T. M. (1996) *Proc. Natl. Acad. Sci. U. S. A.* **93,** 8407–8412
21. Szczesna-Skorupa, E., Mallah, B., and Kemper, B. (2003) *J. Biol. Chem.* **278,** 31269–31276
22. Ghosh, A. K., Pretzer, E., Cho, H., Hussain, K. A., and Duzgunes, N. (2002) *Antiviral Res.* **54,** 29–36
23. Ghosh, A. K., Leshchenko, S., and Noetzel, M. (2004) *J. Org. Chem.* **69,** 7822–7829
24. Koh, Y., Nakata, H., Maeda, K., Ogata, H., Bilcer, G., Devasamudram, T., Kincaid, J. F., Boross, P., Wang, Y. F., Tie, Y., Volarath, P., Gaddis, L., Harrison, R. W., Weber, I. T., Ghosh, A. K., and Mitsuya, H. (2003) *Antimicrob. Agents Chemother.* **47,** 3123–3129
25. Kovalevsky, A. Y., Liu, F., Leshchenko, S., Ghosh, A. K., Louis, J. M., Harrison, R. W., and Weber, I. T. (2006) *J. Mol. Biol.* **363,** 161–173
26. Ghosh, A. K., Sridhar, P. R., Leshchenko, S., Hussain, A. K., Li, J., Kovalevsky, A. Y., Walters, D. E., Wedekind, J. E., Grum-Tokars, V., Das, D., Koh, Y., Maeda, K., Gatanaga, H., Weber, I. T., and Mitsuya, H. (2006) *J. Med. Chem.* **49,** 5252–5261
27. Maibaum, J., and Rich, D. H. (1988) *J. Med. Chem.* **31,** 625–629

AQ: M

28. Miyawaki, A., Llopis, J., Heim, R., McCaffery, J. M., Adams, J. A., Ikura, M., and Tsien, R. Y. (1997) *Nature* **388,** 882–887
29. Babe, L. M., Rose, J., and Craik, C. S. (1992) *Protein Sci.* **1,** 1244–1253
30. Ishima, R., Torchia, D. A., Lynch, S. M., Gronenborn, A. M., and Louis, J. M. (2003) *J. Biol. Chem.* **278,** 43311–43319
31. Ishima, R., Ghirlando, R., Tozser, J., Gronenborn, A. M., Torchia, D. A., and Louis, J. M. (2001) *J. Biol. Chem.* **276,** 49110–49116
32. Louis, J. M., Ishima, R., Nesheiwat, I., Pannell, L. K., Lynch, S. M., Torchia, D. A., and Gronenborn, A. M. (2003) *J. Biol. Chem.* **278,** 6085–6092
33. Yoshimura, K., Kato, R., Kavlick, M. F., Nguyen, A., Maroun, V., Maeda, K., Hussain, K. A., Ghosh, A. K., Gulnik, S. V., Erickson, J. W., and Mitsuya, H. (2002) *J. Virol.* **76,** 1349–1358
34. Patick, A. K., Mo, H., Markowitz, M., Appelt, K., Wu, B., Musick, L., Kalish, V., Kaldor, S., Reich, S., Ho, D., and Webber, S. (1996) *Antimicrob. Agents Chemother.* **40,** 292–297
35. Konvalinka, J., Litterst, M. A., Welker, R., Kottler, H., Rippmann, F., Heuser, A. M., and Krausslich, H. G. (1995) *J. Virol.* **69,** 7180–7186
36. Amano, M., Koh, Y., Das, D., Li, J., Leschenko, S., Wang, Y. F., Boross, P. I., Weber, I. T., Ghosh, A. K., and Mitsuya, H. (2007) *Antimicrob. Agents Chemother.* **51,** 2143–2155
37. Miller, J. F., Andrews, C. W., Brieger, M., Furfine, E. S., Hale, M. R., Hanlon, M. H., Hazen, R. J., Kaldor, I., McLean, E. W., Reynolds, D., Sammond, D. M., Spaltenstein, A., Tung, R., Turner, E. M., Xu, R. X., and Sherrill, R. G. (2006) *Bioorg Med. Chem. Lett.* **16,** 1788–1794
38. Hicks, C. B., Cahn, P., Cooper, D. A., Walmsley, S. L., Katlama, C., Clotet, B., Lazzarin, A., Johnson, M. A., Neubacher, D., Mayers, D., and Valdez, H. (2006) *Lancet* **368,** 466–475
39. Maeda, K., Nakata, H., Koh, Y., Miyakawa, T., Ogata, H., Takaoka, Y., Shibayama, S., Sagawa, K., Fukushima, D., Moravek, J., Koyanagi, Y., and Mitsuya, H. (2004) *J. Virol.* **78,** 8654–8662
40. Tie, Y., Boross, P. I., Wang, Y. F., Gaddis, L., Hussain, A. K., Leshchenko, S., Ghosh, A. K., Louis, J. M., Harrison, R. W., and Weber, I. T. (2004) *J. Mol. Biol.* **338,** 341–352
41. Thaisrivongs, S., Skulnick, H. I., Turner, S. R., Strohbach, J. W., Tommasi, R. A., Johnson, P. D., Aristoff, P. A., Judge, T. M., Gammill, R. B., Morris, J. K., Romines, K. R., Chrusciel, R. A., Hinshaw, R. R., Chong, K. T., Tarpley, W. G., Poppe, S. M., Slade, D. E., Lynn, J. C., Horng, M. M., Tomich, P. K., Seest, E. P., Dolak, L. A., Howe, W. J., Howard, G. M., Watenpaugh, K. D., *et al.* (1996) *J. Med. Chem.* **39,** 4349–4353 AQ: N
42. Kovalevsky, A. Y., Tie, Y., Liu, F., Boross, P. I., Wang, Y. F., Leshchenko, S., Ghosh, A. K., Harrison, R. W., and Weber, I. T. (2006) *J. Med. Chem.* **49,** 1379–1387
43. Muzammil, S., Armstrong, A. A., Kang, L. W., Jakalian, A., Bonneau, P. R., Schmelmer, V., Amzel, L. M., and Freire, E. (2007) *J. Virol.* **81,** 5144–5154
44. Prabu-Jeyabalan, M., Nalivaika, E. A., Romano, K., and Schiffer, C. A. (2006) *J. Virol.* **80,** 3607–3616
45. De Meyer, S., Azijn, H., Surleraux, D., Jochmans, D., Tahri, A., Pauwels, R., Wigerinck, P., and de Bethune, M. P. (2005) *Antimicrob. Agents Chemother.* **49,** 2314–2321
46. Poveda, E., Blanco, F., Garcia-Gasco, P., Alcolea, A., Briz, V., and Soriano, V. (2006) *AIDS* **20,** 1558–1560
47. Youle, M., Staszweski, S., Clotet, B., Arribas, J. R., Blaxhult, A., Carosi, G., Dejesus, E., Di Perri, G., Estrada, V., Fisher, M., Kovacs, C., Kulasegaram, R., Lazzarin, A., Marriott, D., Munoz, L., Reynes, J., Shalit, P., Slim, J., Tsoukas, C., Vaccaro, A., and Vera, J. (2006) *HIV Clin. Trials* **7,** 86–96
48. Hoetelmans, R., Van der Sandt, I., De Pauw, M., Struble, K., Peeters, M., and Van der Geest, R. (2003) *10th Conference on Retroviruses and Opportunistic Infections (CROI),* Feb 10–14, 549 (Abstr.) AQ: O

ANTIMICROBIAL AGENTS AND CHEMOTHERAPY, Aug. 2007, p. 2701–2708 Vol. 51, No. 8
0066-4804/07/$08.00+0 doi:10.1128/AAC.00277-07


# Activity against Human Immunodeficiency Virus Type 1, Intracellular Metabolism, and Effects on Human DNA Polymerases of 4′-Ethynyl-2-Fluoro-2′-Deoxyadenosine▽

Hirotomo Nakata,[1,2,3] Masayuki Amano,[1,2] Yasuhiro Koh,[1,2] Eiichi Kodama,[4] Guangwei Yang,[5] Christopher M. Bailey,[5] Satoru Kohgo,[6] Hiroyuki Hayakawa,[6] Masao Matsuoka,[4] Karen S. Anderson,[5] Yung-Chi Cheng,[5] and Hiroaki Mitsuya[1,2,3]*

*Department of Infectious Diseases[1] and Department of Hematology,[2] Kumamoto University School of Medicine, Kumamoto 860-8556, Japan; Experimental Retrovirology Section, HIV and AIDS Malignancy Branch, National Cancer Institute, National Institutes of Health, Bethesda, Maryland 20892[3]; Laboratory of Virus Immunology, Institute for Virus Research, Kyoto University, Kyoto 606-8507, Japan[4]; Department of Pharmacology, Yale University School of Medicine, New Haven, Connecticut 06520[5]; and Biochemicals Division, Yamasa Corporation, Chosi 288-0056, Japan[6]*

Received 23 February 2007/Returned for modification 13 April 2007/Accepted 24 May 2007

**We examined the intracytoplasmic anabolism and kinetics of antiviral activity against human immunodeficiency virus type 1 (HIV-1) of a nucleoside reverse transcriptase inhibitor, 4′-ethynyl-2-fluoro-2′-deoxyadenosine (EFdA), which has potent activity against wild-type and multidrug-resistant HIV-1 strains. When CEM cells were exposed to 0.1 μM [$^3$H]EFdA or [$^3$H]3′-azido-2′,3′-dideoxythymidine (AZT) for 6 h, the intracellular EFdA-triphosphate (TP) level was 91.6 pmol/$10^9$ cells, while that of AZT was 396.5 pmol/$10^9$ cells. When CEM cells were exposed to 10 μM [$^3$H]EFdA, the amount of EFdA-TP increased by 22-fold (2,090 pmol/$10^9$ cells), while the amount of [$^3$H]AZT-TP increased only moderately by 2.4-fold (970 pmol/$10^9$ cells). The intracellular half-life values of EFdA-TP and AZT-TP were ~17 and ~3 h, respectively. When MT-4 cells were cultured with 0.01 μM EFdA for 24 h, thoroughly washed to remove EFdA, further cultured without EFdA for various periods of time, exposed to HIV-$1_{NL4-3}$, and cultured for an additional 5 days, the protection values were 75 and 47%, respectively, after 24 and 48 h with no drug incubation, while those with 1 μM AZT were 55 and 9.2%, respectively. The 50% inhibitory concentration values of EFdA-TP against human polymerases α, β, and γ were >100 μM, >100 μM, and 10 μM, respectively, while those of ddA-TP were >100 μM, 0.2 μM, and 0.2 μM, respectively. These data warrant further development of EFdA as a potential therapeutic agent for those patients who harbor wild-type HIV-1 and/or multidrug-resistant variants.**

Highly active antiretroviral therapy (HAART) has had a major impact on the AIDS epidemic in industrially advanced nations. However, eradication of human immunodeficiency virus type 1 (HIV-1) does not appear to be currently possible, in part due to the viral reservoirs remaining in blood and infected tissues. Moreover, a number of challenges have been encountered in the antiviral therapy of HIV-1 infection (7, 24, 25). Challenges include (i) various acute to long-term drug-related toxicities; (ii) only a partial restoration of immunologic functions is achieved once HIV-infected individuals develop AIDS; (iii) the development of various cancers as a consequence of survival prolongation with HAART; (iv) flare-ups of inflammation in individuals receiving HAART, i.e., the immune reconstruction syndrome (IRS); and (v) the increased cost of antiviral therapy.

Successful antiviral drugs, in theory, exert their virus-specific effects by interacting with viral receptors, virally encoded enzymes, viral structural components, or viral genes or their transcripts without disturbing cellular metabolism or function (19). However, at present, no antiretroviral drugs or agents are likely to be completely specific for HIV-1 or devoid of toxicity or adverse effects in the therapy of AIDS, which has been a critical issue because patients with AIDS and its related diseases will have to receive antiretroviral therapy for a long period of time, perhaps for the rest of their lives. Thus, the identification of a new class of antiretroviral drugs that have a unique mechanism(s) of action, that are highly potent to drug-resistant HIV-1 variants, that delay or do not allow the emergence of drug-resistant variants, and that produce no or minimal adverse effects remains an important therapeutic objective.

We recently designed and synthesized a number of 4′-ethynyl (4′-*E*)-2′-deoxynucleosides and their analogs (EdNs) and identified a series of potent anti-HIV-1 compounds which blocked the replication of a wide spectrum of laboratory and clinical HIV-1 strains in vitro (14, 21). These EdN analogs, unlike the existing Food and Drug Administration (FDA)-approved nucleoside reverse transcriptase inhibitors, possess a 3′-OH in their sugar moiety; however, they cause viral DNA chain termination, resulting in reverse transcriptase inhibition (14, 23). Through our optimization efforts of such 4′-*E* nucleoside analogs, we have now identified 4′-*E*-2-fluoro-2′-deoxyadenosine (EFdA), which exerts highly potent anti-HIV activity with favorable in vitro cell toxicities.

In the present study, we determined the profiles of antiviral activity and cell toxicity of EFdA and further examined its

* Corresponding author. Mailing address: Departments of Infectious Diseases and Hematology, Kumamoto University School of Medicine, 1-1-1 Honjo, Kumamoto 860-8556, Japan. Phone: 81 96-373-5156. Fax: 81 96-363-5265. E-mail: hm21q@nih.gov.

▽ Published ahead of print on 4 June 2007.

cellular uptake, intracytoplasmic anabolism, and kinetics of antiviral activity against various HIV-1 strains. The present data suggest that EFdA represents a potent anti-HIV-1 agent with the possibility of a once- or twice-a-day regimen and warrants further development as a potential therapeutic agent for those harboring wild-type HIV-1 and/or multidrug resistant variants.

## MATERIALS AND METHODS

**Antiviral agents and radiochemicals.** EFdA was newly designed, synthesized, and tested for anti-HIV-1 activity in vitro. A method for the synthesis of EFdA will be published elsewhere. The structure of EFdA is illustrated in Fig. 1. 3′-Azido-2′,3′-deoxythymidine (AZT or zidovudine) was purchased from Sigma (St. Louis, MO). Saquinavir (SQV) and amprenavir (APV) were kindly provided by Roche Products Ltd. (Welwyn Garden City, United Kingdom) and Glaxo-SmithKline (Research Triangle Park, Durham, NC), respectively. Tenofovir (TDF) was obtained from the National Institutes of Health AIDS Research and Reference Reagent Program. [*methyl*-$^3$H]AZT (specific radioactivity, 12 Ci/mmol) and [8-$^3$H]EFdA (specific radioactivity, 5 Ci/mmol) were obtained from Moravek Biochemicals, Inc. (Brea, CA).

**Cells and viruses.** CEM and MT-4 cells were grown in RPMI 1640-based culture medium supplemented with 15% fetal calf serum (FCS; HyClone Laboratories, Logan, UT), 50 U of penicillin per ml, and 50 μg of streptomycin per ml. The HeLa-CD4-LTR-β-gal indicator cell line expressing human CCR5 (CCR5$^+$-MAGI [multinuclear activation of a galactosidase indicator]) (17) was a kind gift from Yosuke Maeda. CCR5$^+$-MAGI cells were maintained in Dulbecco's modified Eagle's medium (DMEM) supplemented with 15% FCS, 200 μg/ml G418, 100 μg/ml hygromycin B, and 100 μg/ml zeomycin. Peripheral blood mononuclear cells (PBMC) isolated from HIV-1-seronegative donors by using Ficoll-Hypaque were cultured in RPMI 1640-based culture medium containing 10% FCS and antibiotics with 10 μg of phytohemagglutinin (PHA-PBMC) for 3 days prior to drug susceptibility assays. HIV-1 strains used for the drug susceptibility assay (see below) were as follows: HIV-$1_{Ba\text{-}L}$, HIV-$1_{NL4\text{-}3}$, and three HIV-1 clinical isolates, HIV-$1_{MDR/C}$, HIV-$1_{MDR/G}$, and HIV-$1_{MDR/MM}$, which were originally isolated from patients with AIDS who had received from 9 to 11 anti-HIV-1 drugs over the previous 32 to 83 months and which were genotypically and phenotypically characterized as multidrug-resistant HIV-1 variants (15, 28).

**Drug susceptibility assay.** The susceptibilities of HIV-$1_{Ba\text{-}L}$, HIV-$1_{NL4\text{-}3}$, and the three multidrug-resistant primary HIV-1 isolates to various drugs were determined as previously described (28), with minor modifications. Briefly, PHA-PBMC ($10^6$ cells/ml) were exposed to 50 50% tissue culture infectious doses of HIV-$1_{Ba\text{-}L}$ or each primary HIV-1 isolate and cultured in the presence or absence of various concentrations of drugs in 10-fold serial dilutions in 96-well microculture plates ($10^5$ cells/well). On day 7 of culture, the supernatant was harvested, and the amount of p24 Gag protein was determined by using a fully automated chemiluminescent enzyme immunoassay system (Lumipulse F; Fujirebio, Inc., Tokyo, Japan) (20). The drug concentrations that suppressed the production of p24 Gag protein by 50% (50% effective concentrations [$EC_{50}$s]) were determined by comparison with the level of p24 production in drug-free control cell cultures. All assays were performed in triplicate. To determine the drug susceptibility of HIV-$1_{NL4\text{-}3}$, a methylthiazoletetrazolium (MTT) assay was used, employing MT-4 cells ($10^4$ cells/well) as target cells, as previously described (1). The cytotoxicity of each drug against MT-4 cells and PBMC was also determined using the MTT assay as previously described (1).

**Uptake and intracellular metabolism of EFdA.** CEM cells ($10^6$ cells/ml) were incubated with various concentrations (0.1, 1, and 10 μM) of [$^3$H]EFdA or [$^3$H]AZT for 6 h, followed by thorough washing to remove extracellular drugs. Subsequently, nucleosides/nucleotides within the cells were extracted with 60% methanol and subjected to high-performance liquid chromatography (HPLC) on an ion exchange Partisil 10-SAX column (Whatman International Ltd., Maidstone, United Kingdom). HPLC analysis was performed according to previously established procedures (18) using two elution buffers, buffer A (0.03 M ammonium phosphate) and buffer B (nine parts of 0.7 M ammonium phosphate and one part 100% ethanol). For elution, the following program was used: 5 min of buffer A, followed by 10 min of a highly convex gradient to 75% buffer A–25% buffer B, followed by 15 min of a slightly convex gradient to 100% buffer B, and finally followed by a 10-min isocratic elution with buffer B. One-minute elution fractions were collected, and the radioactivity of each fraction was measured using a liquid scintillation counter to determine the amount of metabolites.

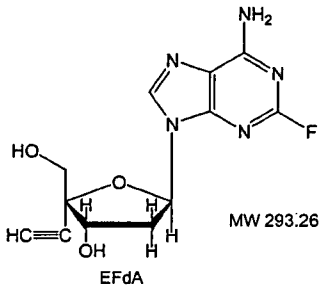


FIG. 1. Structure of EFdA.

**Determination of the amount of EFdA and its metabolites within human CD4$^+$ T cells.** Human CD4$^+$ CEM and MT-4 cells ($10^6$ cells/ml) were incubated with 200 nM [$^3$H]EFdA or [$^3$H]AZT for 6 h, thoroughly washed, and further cultured without the addition of EFdA or AZT, followed by the extraction of nucleosides/nucleotides with 60% methanol at various time periods of culture (2, 4, 8, 12, and 24 h). The amounts of intracellular metabolites were determined by HPLC analysis as described above.

**In vitro persistence of anti-HIV activity of EFdA.** MT-4 cells ($10^5$ cells/ml) were exposed to a concentration of 0.01, 0.1, or 1 μM EFdA, AZT, or TDF for 24 h, thoroughly washed to deplete extracellular drugs, cultured for various periods of time (0, 2, 6, 12, 24, and 48 h), exposed to HIV-$1_{NL4\text{-}3}$, and further cultured for 5 days. On day 5, the amount of p24 antigen produced in the culture medium was determined to monitor the anti-HIV-1 activity, as described above. The MTT assay was performed, employing PBMC ($10^6$ cells/ml) and HIV-$1_{Ba\text{-}L}$ under the same conditions as described above, and the activity of the drug to block the cytopathic effect of the virus was evaluated.

An additional assay was performed using CCR5$^+$-MAGI cells (the MAGI assay) under the same conditions as described above, using HIV-$1_{Ba\text{-}L}$ in place of HIV-$1_{NL4\text{-}3}$ and the final culture after 48 h instead of 5 days of culture. The MAGI assay was conducted as previously described (16). Briefly, CCR5$^+$-MAGI cells were plated ($10^4$ cells/well) and cultured in 96-well, flat-bottomed microculture plates. After 24 h of incubation, the cells were exposed to various concentrations of a test compound and HIV-1 in DMEM containing 15% FCS and were stained at 48 h of culture with chlorophenol red β-D-galactopyranoside. Supernatants were removed, and the cells were lysed with 100 μl of phosphate-buffered saline containing 1% Triton X-100. A solution (100 μl) containing 10 mM chlorophenol red β-D-galactopyranoside, 2 mM $MgCl_2$, and 0.1 M $KH_2PO_4$ was added to each well, the mixture was incubated at room temperature in the dark for 30 min, and the optical density (wavelength, 570 nm) was measured in a microplate reader ($V_{max}$; Molecular Devices, Sunnyvale, CA).

**Determination of EFdA-TP effects on human DNA polymerases α, β, and γ.** Human DNA polymerases α and β were obtained from Terasa Wang at Stanford University and Joann B. Sweasy at Yale University, respectively. Human DNA polymerase γ was purified by Anderson as previously described (2). In the steady-state enzymatic assay, a DNA primer/template of 21 and 36 nucleotides ($D_{21}/D_{36}$) and activated calf thymus DNA were employed. The sequences of $D_{21}/D_{36}$ were 5′-TCA GGT CCC TGT TCG GGC GCC-3′ (primer) and 3′-CGA AAG TCC AGG GAC AAG CCC GCG GTG ACG ATC TCT-5′ (template), respectively.

In the assay of polymerase activity inhibition, the reaction mixture used was as follows: 50 mM Tris (pH 8.0), 8 mM $MgCl_2$, 60 mM KCl, 10 mM dithiothreitol, 30 μg/ml bovine serum albumin, 250 nM $D_{21}/D_{36}$ or 0.1 mg/ml calf thymus DNA as the DNA primer/template, 0.3 μM dATP (α-$^{32}$P labeled), 1 unit DNA polymerase α (defined as the amount of polymerase α that incorporated 1 pmol of $^{32}$P-labeled dATP into calf thymus DNA at 37°C in 30 min), 100 nM polymerase β or 2.5 nM polymerase γ, and various concentrations of EFdA-TP or ddA-TP as the inhibitor. The reaction was performed at 37°C for 30 min and was stopped by adding 0.5 M EDTA. Subsequently, the reaction mixture was dotted onto DE81 filter paper. After each dotted filter paper was washed three times with 0.5 M sodium phosphate buffer, the paper was subjected to phosphorimaging analysis, and the polymerase activity was determined by quantifying the amount of incorporated dAMP (27).

**Determination of $K_i$ values for EFdA-TP inhibition of human polymerase γ.** For steady-state inhibition assays, a final concentration of 10 nM human polymerase γ catalytic subunit, 50 nM human polymerase γ accessory subunit, 2.5 mM $MgCl_2$, 1 μM $D_{21}/D_{36}$, and various concentrations of [α-$^{32}$P]dATP were used. These conditions were determined to be in the linear phase at steady state

TABLE 1. Anti-HIV-1 activity of EfdA

| Drug | $EC_{50}$ value (μM ± SD) for the strains shown (fold change)[a] | | | | | $CC_{50}$ value (μM) for: | |
|---|---|---|---|---|---|---|---|
| | R5-HIV-$1_{Ba-L}$ | R5-HIV-$1_{MDR/MM}$[b] | X4-HIV-$1_{NL4-3}$ | X4-HIV-$1_{MDR/C}$[b] | X4-HIV-$1_{MDR/G}$[b] | MT-4 cells | PHA-PBMC cells |
| EFdA | 0.0004 ± 0.00007 (1) | 0.003 ± 0.0005 (8) | 0.001 ± 0.0002 (1) | 0.004 ± 0.001 (4) | 0.021 ± 0.008 (21) | 11 | 12 |
| AZT | 0.015 ± 0.004 (1) | 0.34 ± 0.008 (22) | 0.033 ± 0.007 (1) | 0.39 ± 0.06 (12) | 0.38 ± 0.09 (12) | >100 | >100 |
| TDF | 0.032 ± 0.006 (1) | 0.082 ± 0.01 (3) | 0.0 ± 0.006 (1) | 0.047 ± 0.01 (2) | 0.087 ± 0.02 (3) | ND[c] | 53 |
| APV | 0.025 ± 0.005 (1) | 0.43 ± 0.03 (17) | 0.024 ± 0.004 (1) | 0.28 ± 0.02 (12) | 0.25 ± 0.03 (10) | >100 | >100 |
| SQV | 0.008 ± 0.004 (1) | 0.22 ± 0.05 (28) | 0.01 ± 0.005 (1) | 0.037 ± 0.004 (4) | 0.026 ± 0.008 (3) | 26 | 78 |

[a] The $EC_{50}$s were determined with PHA-PBMC, by the inhibition of p24 Gag protein production by the drug as an end point. For HIV-$1_{NL4-3}$, MT-4 cells were exposed to the virus, and the $EC_{50}$ values were determined using the MTT assay. All assays were conducted in duplicate or triplicate, and the data shown represent means ± 1 standard deviation (SD) derived from the results of two independent experiments. Numbers in parentheses represent changes in $EC_{50}$s for each isolate compared to the $EC_{50}$s for HIV-$1_{Ba-L}$ and HIV-$1_{NL4-3}$.

[b] Strains HIV-$1_{MDR/C}$, HIV-$1_{MDR/G}$, and HIV-$1_{MDR/MM}$ were isolated from patients who had received antiretroviral therapy for long periods of time and whose virus strains had acquired a number of mutations in the RT- and PR-encoding HIV-1 genes. The amino acid substitutions identified for the RT-encoding regions of HIV-$1_{MDR/MM}$, HIV-$1_{MDR/C}$, and HIV-$1_{MDR/G}$ compared to the consensus type B sequences cited from the Los Alamos database include M41L, D67N, T69D, D123E, M184V, G196R, L210W, L214F and T215Y, M41L, E44D, D67N, T69D, A98S, D123E, D177E, M184V, L210W, R211K, L214F, T215F, K219Q and L228H, and D67G, S68G, T69D, K70R, V118I, E122K, I135T, M184V, Q197K, T125F, D218E, and K219Q, respectively.

[c] ND, not done.

after 2 min. Premixed solutions of dATP, $MgCl_2$, and various concentrations of an inhibitor were mixed with the enzyme and $D_{21}/D_{36}$ to initiate the reaction. After 2 min, each reaction was quenched with a final concentration of 0.3 M EDTA. A constant amount of 5′-radiolabeled $D_{36}$ was added at the end of the reaction to normalize for loading. Products were then analyzed by 20% polyacrylamide gel electrophoresis and analyzed on a Bio-Rad Molecular Imager FX. The amount of product was determined as the fraction of the elongated primer ($D_{22}$) divided by the radiolabeled template ($D_{36}$). Michaelis-Menten curves were generated, and the apparent $V_{max}$ and $K_m$ values for substrate in the presence of various concentrations of the inhibitor were determined. Nonlinear regression was then performed, fitting the curves for competitive inhibition to provide the $K_i$ value for EFdA-TP (Table 2). The values of $K_m$ for dATP and $K_{cat}$ were also determined.

## RESULTS

**Anti-HIV-1 activity and cytotoxicity of EFdA.** Certain 4′-ethnyl-2′-deoxynucleoside analogs exert potent activity against a wide spectrum of HIV-1 strains including the multidrug resistant (MDR) HIV-1 variants and the HIV-1 strains as previously described (14). In an attempt to optimize the anti-HIV-1 activity, we generated a number of 4′-ethynyl-containing congeners and identified EFdA as one of the most potent and least toxic nucleoside analogs. As shown in Table 1, in the evaluation of the activity of EFdA against HIV-1 variants, we employed three primary HIV-1 strains isolated from patients for whom existing anti-HIV-1 regimens had failed after they had received from 9 to 11 anti-HIV-1 drugs over 32 to 83 months (15, 28). These MDR strains contained amino acid substitutions in the reverse transcriptase- and protease-encoding regions, which have reportedly been associated with HIV-1 resistance. EFdA blocked the replication of five HIV-1 strains, (X4-HIV-$1_{NL4-3}$, X4-HIV-$1_{MDR/C}$, X4-HIV-$1_{MDR/G}$, R5-HIV-$1_{Ba-L}$, and R5-HIV-$1_{MDR/MM}$), with $EC_{50}$ values ranging from 0.0004 to 0.021 μM (Table 1). The $EC_{50}$ value change of EFdA (21-fold) against HIV-$1_{MDR/G}$ is greater than that of AZT (12-fold). However, it should be noted that against all MDR HIV-1 variants examined, the absolute $EC_{50}$ values of EFdA remained the lowest compared to those of four representative FDA-approved antiviral agents (AZT, TDF, APV, and SQV). Although EFdA's 50% cytotoxicity concentration ($CC_{50}$, the concentration of a compound that reduces the number of cells by 50%) value was relatively low (11 μM for MT-4 cells and 12 μM for PHA-PBMC) compared to that of AZT and APV (both were >100 μM), the selectivity indices of EFdA with X4-HIV-$1_{NL4-3}$ and R5-HIV-$1_{Ba-L}$ were 11,000 and 27,500, respectively, indicating that EFdA had a relatively favorable cytotoxicity profile compared to those of AZT and APV, whose selectivity indices were >3,030 and >3,571 with X4-HIV-$1_{NL4-3}$ and >6,667 and >4,000 with R5-HIV-$1_{Ba-L}$, respectively.

**Intracellular metabolism of EFdA.** In order to characterize the profile of intracellular metabolism of EFdA, we tritiated EFdA ([$^3$H]EFdA) and determined the amounts of intracellular metabolites of [$^3$H]EFdA in human CD4$^+$ CEM cells. CEM cells were cultured in the presence of 0.1, 1, and 10 μM [$^3$H]EFdA for 6 h, and intracellular nucleosides/nucleotides were extracted with 60% methanol as previously described (18). The extracted samples containing [$^3$H]EFdA metabolites were subjected to HPLC, and the radioactivity of each eluted sample was determined and plotted as a function of elution time. The identity of each peak of [$^3$H]EFdA metabolite was determined by comparison with the known elution times of unlabeled EFdA-MP, EFdA-DP, and EFdA-TP. The amount of the specific metabolite was determined as the sum of the radioactivity for its peak plus the activity for two flanking 1-min fractions.

First, we examined the uptake of EFdA into CEM cells when cultured in the presence of 0.1 μM [$^3$H]EFdA for 6 h by determining the area under the radioactivity curve, which added up to 1,731 pmol/$10^9$ cells. In contrast, the uptake level of AZT was greater than that of EFdA by approximately 2.5-fold (4,349 pmol/$10^9$ cells), when determined with CEM cells exposed to 0.1 μM [$^3$H]AZT.

Among the three distinct peaks, representing EFdA-MP, -DP, and -TP, seen with 0.1 μM EFdA exposure (Fig. 2A), the amount of EFdA-TP was comparable to that of EFdA-MP and greater than that of EFdA-DP. When the cells were exposed to higher concentrations (1 and 10 μM) of [$^3$H]EFdA, the amounts of all three EFdA phosphates increased proportionately (Fig. 2B). This profile of EFdA phosphates contrasted with that of AZT phosphates in cells exposed to 0.1 μM [$^3$H]AZT (Fig. 2C), in which the amount of AZT-MP was

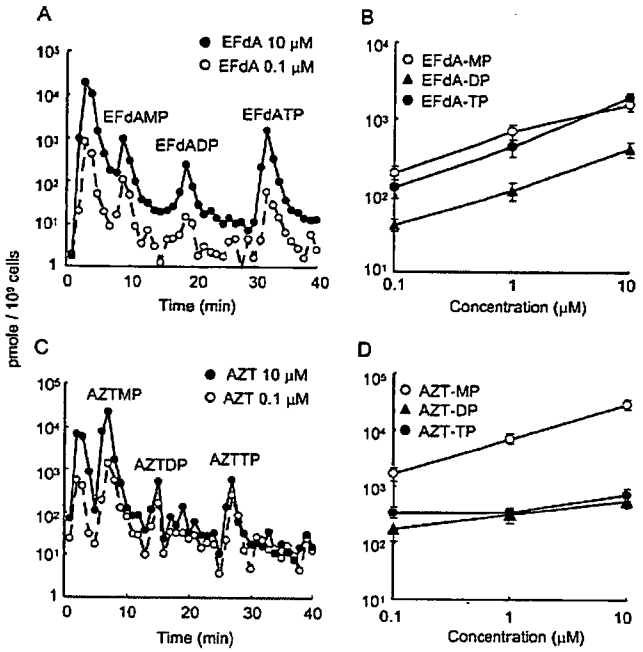


FIG. 2. Cellular uptake and intracellular phosphorylation profiles of EFdA. CEM cells ($10^6$ cells/ml) were incubated in the presence of various concentrations (0.1, 1, and 10 μM) of [$^3$H]EFdA or [$^3$H]AZT for 6 h and washed, and intracellular nucleosides/nucleotides were extracted with 60% methanol. The extracts were subjected to HPLC. One-minute fractions were collected until 40 min, and the radioactivity of the collected samples was determined with a scintillation counter for EFdA (A) and AZT (C). The radioactivity of the sample showing each peak and its flanking samples' radioactivity (total of 3-min fractions) were summed and plotted for EFdA (B) and AZT (D). For the sake of clarity, the profiles of [$^3$H]EFdA and [$^3$H]AZT metabolites in the cells exposed to 1 μM of each agent have been omitted from panels A and C. Determination of intracellular phosphorylation profiles of EFdA and AZT was conducted on two independent occasions, and comparable profiles were obtained in those two experiments. Shown in panels A and C are representative data. The data shown in panels B and D are geometric means ± 1 standard deviation.

greater than that of AZT-DP or AZT-TP, in agreement with previous observations by Furman et al. (8) and Balzarini et al. (3). When the cells were exposed to 1 and 10 μM [$^3$H]AZT, the amounts of AZT-MP increased disproportionately in comparison with those of AZT-DP and -TP. The increase of EFdA-TP level from 0.1 to 10 μM exposure was 22-fold, while that of the AZT-TP level was only 2.4-fold. The ratio of EFdA-TP to EFdA-MP with 10 μM exposure was 1.5, while that of AZT-TP to AZT-MP was 0.031. The high EFdA-TP/EFdA-MP ratio indicates that EFdA is highly efficiently phosphorylated to produce EFdA-TP and/or that EFdA-TP, once formed, is substantially stable intracellularly. The significant intracellular accumulation of AZT-MP and the small amount of AZT-TP are in agreement with previous observations that AZT-MP is a relatively poor substrate for human thymidylate kinase and that the transition of AZT-MP to AZT-DP is substantially delayed (8).

**Intracellular persistence of phosphates of EFdA-TP.** We therefore determined the intracellular stability of each species of EFdA phosphate. When CD4$^+$ CEM cells were cultured with 200 nM [$^3$H]EFdA for 6 h and the amount of each of the phosphates was determined at various time points following thorough washing of the cells, the intracellular levels of all forms of EFdA phosphates persisted longer than those of AZT phosphates (Fig. 3A). As determined at 8 h after EFdA removal, intracellular levels of EFdA-MP, -DP, and -TP had remained, with 50%, 45%, and 72%, respectively, of the values at 0 h, while intracellular levels of AZT-MP, -DP, and -TP rapidly decreased to 16%, 26%, and 26%, respectively. As determined at 24 h after drug removal, intracellular levels of AZT-MP, -DP, and -TP were 31, 23, and 38%, respectively, for EFdA and 10, 11, and 9%, respectively, for AZT. Moreover, the data showed that the half-life ($t_{1/2}$) values of EFdA-MP, -DP, and -TP were 8.1, 6.7, and 17.2 h, respectively, while those of AZT-MP, -DP, and -TP were 1.4, 1.6, and 2.8 h, respectively, indicating that the intracellular half-lives of all three EFdA phosphates are significantly longer than those of AZT phosphates. The profiles of EFdA and AZT phosphorylation determined with another human CD4$^+$ MT-4 T-cell line were similar to those obtained with CEM cells (Fig. 3B).

**Persistent antiviral activity of EFdA after EFdA removal in culture.** Since EFdA-TP was present persistently (at a $t_{1/2}$ of ~17 h) in the cytoplasm of human CD4$^+$ T cells, as described above, we asked whether the antiviral activity of EFdA against HIV-1 persisted after EFdA removal from the culture in comparison to the persistence activities of AZT and TDF. MT-4 cells were cultured in the presence of EFdA, AZT, or TDF for 24 h, thoroughly washed, and exposed to HIV-$1_{NL4-3}$ for 0, 2, 6, 12, 24, and 48 h following EFdA removal, and the magnitude of HIV-$1_{NL4-3}$ replication inhibition was determined using p24 amounts in the culture as a readout. As shown in Fig. 4A, when MT-4 cells were pretreated with 0.01 μM EFdA, representing an EFdA concentration 10-fold greater than its $EC_{50}$ value with MT-4 cells (Table 1), the percentages of protection values in the cells exposed to HIV-$1_{NL4-3}$ at post-24 and -48 h were 75 and 47%, respectively. To comparatively evaluate the persistence of the antiviral activity of EFdA as observed above, we tested the persistence of the activity of TDF, which can be administered once daily in clinical settings, under the same conditions. When MT-4 cells were pretreated with 1 μM TDF, representing a TDF concentration 34-fold greater than its $EC_{50}$ value with MT-4 cells (Table 1), the percentages of protection values at post-24 and -48 h were 90 and 64%, respectively. In contrast, in MT-4 cells pretreated with 1 μM AZT, representing an AZT concentration 33-fold greater than its $EC_{50}$ value (Table 1), the percentages of protection values in the cells exposed to HIV-$1_{NL4-3}$ at post-24 and -48 h were 55 and 9.2%, respectively. When we examined the persistence of antiviral activity of EFdA using another target, PBMC or CCR5$^+$-MAGI cells, and HIV-$1_{Ba-L}$, the protection by EFdA also appeared to be more persistent than that of AZT (Fig. 4B and C). These results corroborated the longer intracellular persistence of EFdA-TP once formed in human CD4$^+$ T cells, as described above (Fig. 3).

**Inhibitory effects of EFdA against human cellular DNA polymerases.** The inhibition of human DNA polymerases by nucleoside reverse transcriptase inhibitors is known to be associated with critical adverse effects including lactic acidosis and peripheral neuropathy (6, 12). We therefore asked whether EFdA had inhibitory effects on human DNA poly-

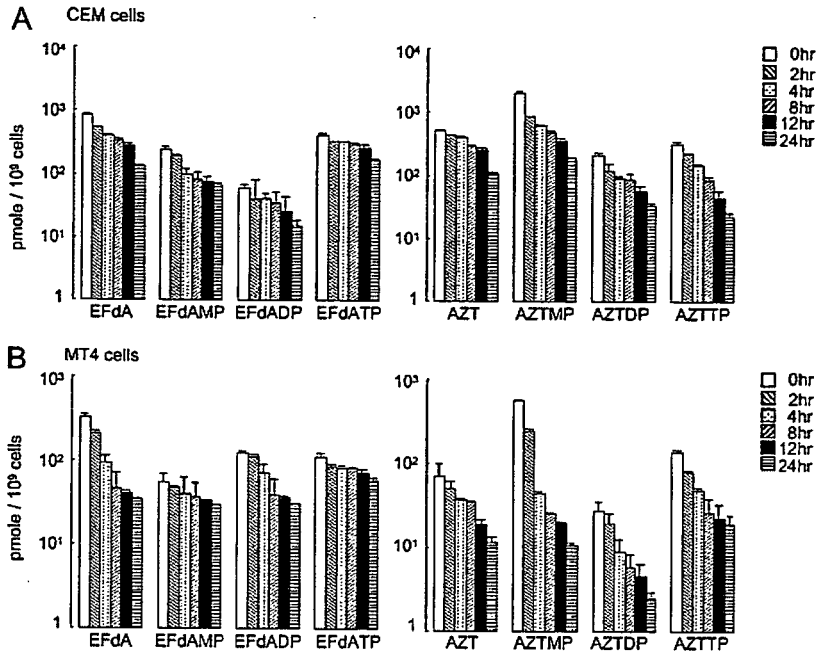


FIG. 3. Intracellular stability of AZT and EFdA metabolites. CEM (A) or MT-4 (B) cells ($10^6$ cells/ml) were incubated with 0.2 μM of [$^3$H]EFdA or [$^3$H]AZT for 6 h and thoroughly washed to remove the extracellular drug. After further incubation of the cells for 0, 2, 4, 8, 12, and 24 h, cell extracts were prepared and subjected to HPLC analysis. Results are shown as arithmetic means of two or three independently conducted experiments (± 1 standard deviation).

merases α, β, and γ. First we determined the 50% inhibitory concentration ($IC_{50}$) values of EFdA-TP and ddA-TP (an active metabolite of didanosine that is, like EFdA, an adenosine congener) against human DNA polymerases α, β, and γ by using calf thymus DNA or a DNA oligomer ($D_{21}/D_{36}$) as the primer/template. Both EFdA-TP and ddA-TP had virtually no inhibition against DNA polymerase α at a concentration of up to 100 μM, as determined with calf thymus DNA (Table 2). EFdA-TP exerted virtually no inhibition against polymerase β, as determined with $D_{21}/D_{36}$ and calf thymus DNA ($IC_{50}$ values were both >100 μM), while ddA-TP had a substantial inhibitory effect, with $IC_{50}$ values of 3 and 0.2 μM, respectively. EFdA-TP also had virtually no inhibition against polymerase γ with $D_{21}/D_{36}$ ($IC_{50}$, >100 μM); however, it was moderately inhibitory against polymerase γ, with an $IC_{50}$ value of 10 μM with calf thymus DNA. In contrast, ddA-TP had substantial inhibitory effects on polymerase γ, using $D_{21}/D_{36}$ or calf thymus DNA, with $IC_{50}$ values of 2 and 0.2 μM, respectively. The $K_i$ values of EFdA-TP and ddA-TP against DNA polymerase γ, as determined with $D_{21}/D_{36}$, were 24.4 ± 7.9 and 4.6 ± 1.7 μM, respectively. These data showed that EFdA-TP had significantly less inhibitory effects on human DNA polymerases than the TP form of the FDA-approved anti-HIV-1 drug, didanosine.

## DISCUSSION

In the present study we demonstrated that EFdA exerts potent activity against a wide range of HIV-1 strains including laboratory and primary strains and highly multidrug-resistant variants, with reasonably low cytotoxicity, as tested in test tubes. In terms of the mechanism of antiviral activity of EFdA, previous reports of 4′-substituted-2′-deoxynucleosides, such as 4′-AZT, have shown that following intracellular anabolism to the 5′ triphosphate, HIV-1 reverse transcriptase (RT) efficiently incorporated the nucleotide, which prevented further chain elongation of the viral DNA (4, 5). Although the rate of incorporation for the 5′-triphosphate of 4′-AZT was quite low, HIV-1 RT was able to incorporate two consecutive molecules efficiently. The subsequent distortion of the growing primer brought about by this incorporation seems to prevent further DNA chain elongation, thus causing delayed chain termination (4, 5). Thus, the salient feature of RT inhibition by 4′-substituted-2′-deoxynucleosides, including EFdA, could be that they cause delayed chain termination, which occurs beyond the polymerase-active site. Indeed, we have recently solved the crystal structure of HIV-1 RT in complex with double-stranded DNA with EFdA-TP (A. Sawani et al., presented at the Retroviruses Conference, Cold Spring Harbor, NY, 22 to 27 May 2007). We found that HIV-1 RT can incorporate EFdA monophosphate at the 3′ end of DNA primers against thymidine. The incorporated EFdA-MP acts as a chain terminator at the point of incorporation, suggesting that RT-catalyzed extension from EFdA-MP primer termini is difficult despite the availability of a free 3′-OH at the inhibitor-terminated primer end. Structural analysis provided insights into unfavorable interactions between the 4′-ethynyl group of the inhibitor-terminated primer and RT residues that may cause inhibition of polymerization.

Considering that the complex antiviral regimens of HAART constitute the major causes of treatment failure and that recent results from multiple clinical trials have shown that a once-

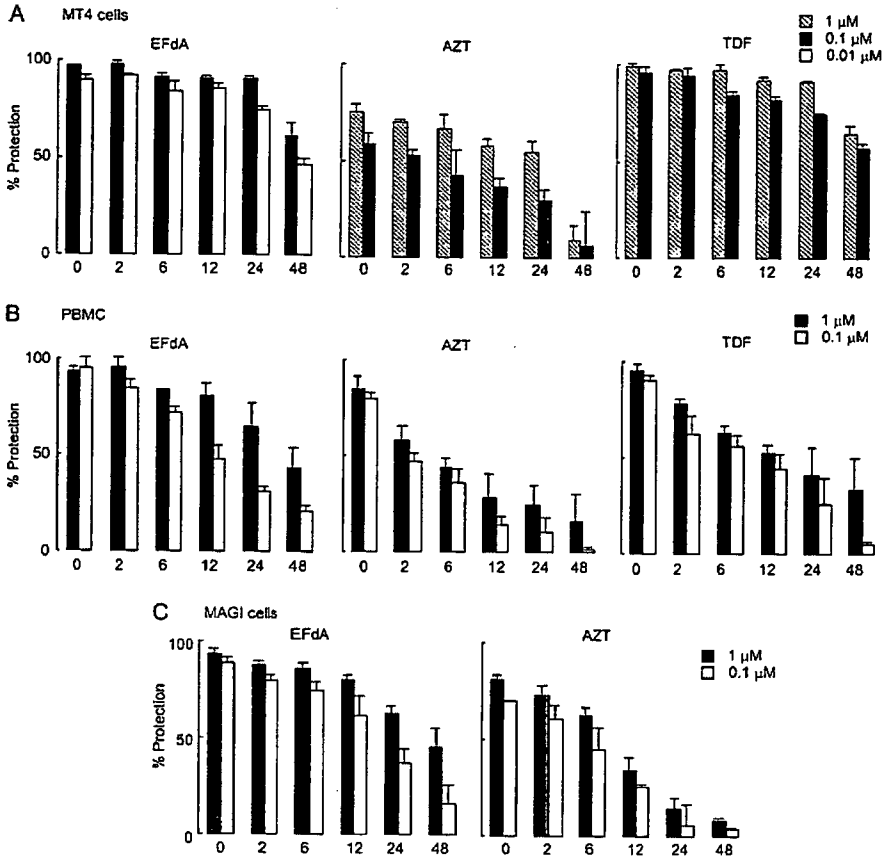


FIG. 4. Persistence of anti-HIV-1 activity after removal of EFdA, AZT, and TDF from culture media. MT-4 (A), PBMC (B), or CCR5$^+$-MAGI cells (C) were exposed to 0.01, 0.1, or 1 μM EFdA (or AZT) for 24 h, thoroughly washed to deplete extracellular drugs, cultured for various periods of time (0, 2, 6, 12, 24, and 48 h), exposed to HIV-1, and further cultured for an additional 5 days with MT-4 cells and PBMC or for an additional 48 h with CCR5$^+$-MAGI cells. Anti-HIV-1 activity was monitored using p24 production or with an MTT assay or a MAGI assay.

daily or twice-daily regimen has produced an improved prognosis (11, 13, 26), we examined whether the pharmacodynamics of EFdA potentially supported a once- or twice-a-day regimen by determining the profiles of anabolic phosphorylation of EFdA in human CD4$^+$ T cells. With regard to the use of these CD4$^+$ human T-cell lines, the intracellular metabolism of certain nucleosides is known to be considerably affected by the status of cells, depending upon proliferation rates, activation states, donors, and other factors (9, 10). It should be noted that the $EC_{50}$ value of EFdA against HIV-$1_{Ba-L}$ determined with PBMC was 0.0004 μM, while that against HIV-$1_{NL4-3}$ determined with MT-4 cells was 0.001 μM. The difference between the values was only a factor of ~3. Thus, we assumed that the phosphorylation pattern and the ratios of EFdA-TP over its possible competitive counterpart, dATP, should be comparable, and we employed two human CD4$^+$ T-cell lines, CEM and MT-4 cells. The present data from these cell lines showed that EFdA efficiently underwent cellular uptake into the cytoplasm and was readily phosphorylated to EFdA-MP, -DP, and -TP (Fig. 2A and B). However, all EFdA phosphates persisted significantly longer than AZT phosphates. Indeed, in both CEM and MT-4 cells exposed to AZT,

TABLE 2. Inhibitory effects of EFdA against DNA polymerase α, β, and γ[a]

| Primer/template | $IC_{50}$ value (μM ± SD) | | | | | $K_i$ value (μM ± SD) of polymerase γ ($D_{21}/D_{36}$) |
|---|---|---|---|---|---|---|
| | Polymerase α (calf thymus DNA) | Polymerase β | | Polymerase γ | | |
| | | $D_{21}/D_{36}$ | Calf thymus DNA | $D_{21}/D_{36}$ | Calf thymus DNA | |
| EFdA-TP | >100 | >100 | >100 | >100 | 10 ± 2 | 24.4 ± 7.9 |
| ddA-TP | >100 | 3 ± 0.3 | 0.2 ± 0.07 | 2 ± 0.3 | 0.2 ± 0.02 | 4.6 ± 1.7 |

[a] In steady-state kinetic assays, DNA primer/template of 21 and 36 nucleotides ($D_{21}/D_{36}$) or activated calf thymus DNA was employed. The $IC_{50}$ values were determined in the presence of 0.3 mM dATP. The $IC_{50}$ values and $K_i$ values represent means ± standard deviations (SD) from two independent experiments. Values of $K_m$ for dATP and $K_{cat}$ were 0.55 ± 0.13 and 0.4 ± 0.03, respectively.

not only the intracellular levels of AZT-DP and AZT-TP but also that of the accumulated AZT-MP rapidly declined in comparison to EFdA phosphates (Fig. 3A and B). These data suggest that AZT phosphates are more vulnerable to intracellular catalysis than EFdA phosphates. The data also suggest that both AZT-MP and -DP get catalyzed without undergoing further phosphorylation. Indeed, the intracellular $t_{1/2}$ of EFdA-TP, an active metabolite of EFdA, was much greater, at 17.2 h, than that of AZT-TP (at 2.8 h) (Fig. 3). It is noteworthy that the intracellular $t_{1/2}$ of the triphosphate forms of d4T, ddC, 3TC, ddI, ABC, and TDF (PMPApp) were reportedly 3.5, 2.6, 10.5 to 15.5, 25 to 40, 3.3, and 15.4 h, respectively (22). Compared with the half-lives of these FDA-approved drugs, EFdA-TP's intracellular half-life (17.2 h) was relatively long, and these results suggest its favorable intracellular pharmacokinetics. We therefore asked whether the longer intracellular persistence of EFdA-TP resulted in more persistent anti-HIV-1 activity of EFdA as EFdA was removed from the culture medium. It was noted that when MT-4 cells were incubated with EFdA (0.1 μM) for 24 h, thoroughly washed to remove EFdA from the culture medium, cultured for various periods of time without adding EFdA, exposed to HIV-1, and further cultured for 5 days, substantial levels of antiviral activity (at post-24- and -48 h, protection values were 91 and 61%, respectively) were seen. The post-24 and -48 h protection values of TDF (0.1 μM), an FDA-approved once-daily anti-HIV-1 drug, were 74 and 57%, respectively (Fig. 4A). In contrast, substantially lower levels of antiviral activity were observed for AZT than for EFdA. When the cells were preincubated with 0.1 μM AZT, only 6% protection was seen with MT-4 cells (Fig. 4). This relatively poor protective activity of AZT should stem from the relatively short $t_{1/2}$ of AZT-TP (8). Thus, the present data that indicate EFdA-TP has a substantially long $t_{1/2}$ of 17 h, in addition to the observed in vitro persistence of antiviral activity, suggest that a once-daily or twice-daily regimen of EFdA is possible.

In regard to the in vitro selection of HIV-1 variants resistant to EFdA, we previously reported that the 3TC resistance-conferring M184V substitution in reverse transcriptase is the major substitution that reduces anti-HIV-1 activity of 4′-ethynyl analogs, although the $EC_{50}$ value change with the M184V substitution was only approximately sixfold (14). In the present work, when we examined MDR HIV-1 variants containing a number of mutations including M184V, the level of resistance was similarly moderate, with changes in their $EC_{50}$ values ranging from 4- to 21-fold (Table 1). However, against such MDR HIV-1 variants, the absolute $EC_{50}$ values remained lowest for EFdA compared to those of four representative FDA-approved antiviral agents (AZT, TDF, APV, and SQV) (Table 1). Thus, it is possible that the "genetic barrier" to HIV-1 acquisition of EFdA resistance can be substantially higher than at least the agents examined in the present study.

It was noted that when cells were exposed to high concentrations (1 and 10 μM) of [$^3$H]EFdA, the amounts of EFdA phosphates increased proportionately (Fig. 2B). This profile of EFdA phosphates contrasted with those of AZT phosphates, which showed that levels of AZT-TP increased only slightly when the cells were exposed to higher concentrations of AZT (Fig. 2D). This phosphorylation profile of AZT stems from the fact that thymidylate kinase has a good affinity for AZT-MP ($K_m$ of ~8 μM), comparable to that of dT-MP ($K_m$ of ~4 μM), while AZT-MP has an extremely low $V_{max}$ value (only 0.3% relative to the $V_{max}$ of dT-MP) (8), resulting in the accumulation of AZT-MP and low levels of AZT-TP. These data suggest that the intracellular anabolic phosphorylation of EFdA to EFdA-TP is substantially efficient, which explains the reason that EFdA exerts such a potent and persistent anti-HIV-1 activity.

As noted above, EFdA was efficiently converted to its active form, EFdA-TP, whose intracellular $t_{1/2}$ was substantially longer (as long as ~17 h) than that of AZT-TP (Fig. 3). However, there was a concern that the long intracellular persistence of EFdA-TP might cause cellular DNA damages, particularly since EFdA retains a 3′-OH group, which may get incorporated into the growing cellular DNA chain, resulting in human DNA chain termination. All the currently available nucleoside reverse transcriptase inhibitors (NRTI) are not devoid of adverse effects such as lactic acidosis and peripheral neuropathy, which are thought to be associated with the interactions of NRTI-TP and cellular DNA polymerases. Therefore, we examined the effects of EFdA-TP on DNA polymerases α, β, and γ, using ddA-TP, the active form of ddI, as a control. EFdA-TP had virtually no significant inhibition against DNA polymerases α and β, although it had moderate inhibitory effects against DNA polymerase γ, with an $IC_{50}$ value of 10 μM when calf thymus DNA was used as a template/primer. The $K_i$ value of EFdA-TP, determined using $D_{21}/D_{36}$ as the template/primer, was 24.4 μM, while that of ddA-TP was 4.6 μM. The anti-HIV-1 drug ddI is known to cause damages in DNA polymerase γ-mediated mitochondrial DNA synthesis, and one can be concerned about the possibility that EFdA may also cause mitochondrial DNA damages since the $K_i$ value (24.4 μM) of EFdA-TP with DNA polymerase γ was only 5.3-fold less than that of ddA-TP (4.6 μM). However, EFdA is much more potent, with an $EC_{50}$ value (~0.0004 μM with PHA-PBMC exposed to HIV-$1_{Ba-L}$ [Table 1]) higher than that of ddI ($EC_{50}$, ~1.5 μM in PHA-PBMC exposed to HIV-$1_{Ba-L}$) (28), and indeed, the ratio of the $K_i$ value to the $IC_{50}$ value for EFdA is as great as 61,000. Thus, EFdA could produce more potent antiviral effects with fewer adverse effects when used as a therapeutic agent for HIV-1 infection and AIDS, although it is important that the antiviral effects and safety of experimental agents be determined only through rigorously controlled preclinical and clinical trials.

## ACKNOWLEDGMENTS

This work was supported in part by a Grant-in-aid for Scientific Research (Priority Areas) from the Ministry of Education, Culture, Sports, Science, and Technology of Japan (Monbu-Kagakusho); by a grant from Promotion of AIDS Research from the Ministry of Health, Welfare, and Labor of Japan (Kosei-Rohdosho, H15-AIDS-001); by a grant from the Cooperative Research Project on Clinical and Epidemiological Studies of Emerging and Re-emerging Infectious Diseases (Renkei Jigyo, no. 78, Kumamoto University) of Monbu-Kagakusho, Kumamoto University Research Program (Kyoten) of Innovative Therapy for AIDS, Emerging and Re-emerging Infectious Diseases; and by the Intramural Research Program of the Center for Cancer Research, National Cancer Institute, National Institutes of Health. This work was also supported in part by NIH grants GM49551 (to K.S.A.) and AI-38204 (to Y.-C.C.).

## REFERENCES


1. **Amano, M., Y. Koh, D. Das, J. Li, S. Leschenko, Y. F. Wang, P. I. Boross, I. T. Weber, A. K. Ghosh, and H. Mitsuya.** 2007. A novel bis-tetrahydrofuranylurethane-containing nonpeptidic protease inhibitor (PI), GRL-98065, is potent against multiple-PI-resistant human immunodeficiency virus in vitro. Antimicrob. Agents Chemother. **51**:2143–2155.
2. **Anderson, K. S.** 2001. The molecular basis of inhibition and toxicity of modified cytosine analogues targetting HIV-1 reverse transcriptase. Antivir. Chem. Chemother. **12**(Suppl.):13–17.
3. **Balzarini, J., L. Naesens, S. Aquaro, T. Knispel, C. Perno, E. De Clercq, and C. Meier.** 1999. Intracellular metabolism of CycloSaligenyl 3'-azido-2', 3'-dideoxythymidine monophosphate, a prodrug of 3'-azido-2', 3'-dideoxythymidine (zidovudine). Mol. Pharmacol. **56**:1354–1361.
4. **Chen, M. S., R. T. Suttmann, E. Papp, P. D. Cannon, M. J. McRoberts, C. Bach, W. C. Copeland, and T. S. Wang.** 1993. Selective action of 4'-azidothymidine triphosphate on reverse transcriptase of human immunodeficiency virus type 1 and human DNA polymerases alpha and beta. Biochemistry **32**:6002–6010.
5. **Chen, M. S., R. T. Suttmann, J. C. Wu, and E. J. Prisbe.** 1992. Metabolism of 4'-azidothymidine. A compound with potent and selective activity against the human immunodeficiency virus. J. Biol. Chem. **267**:257–260.
6. **Coghlan, M. E., J. P. Sommadossi, N. C. Jhala, W. J. Many, M. S. Saag, and V. A. Johnson.** 2001. Symptomatic lactic acidosis in hospitalized antiretroviral-treated patients with human immunodeficiency virus infection: a report of 12 cases. Clin. Infect. Dis. **33**:1914–1921.
7. **De Clercq, E.** 2002. Strategies in the design of antiviral drugs. Nat. Rev. Drug Discov. **1**:13–25.
8. **Furman, P. A., J. A. Fyfe, M. H. St Clair, K. Weinhold, J. L. Rideout, G. A. Freeman, S. N. Lehrman, D. P. Bolognesi, S. Broder, H. Mitsuya, et al.** 1986. Phosphorylation of 3'-azido-3'-deoxythymidine and selective interaction of the 5'-triphosphate with human immunodeficiency virus reverse transcriptase. Proc. Natl. Acad. Sci. USA **83**:8333–8337.
9. **Gao, W. Y., R. Agbaria, J. S. Driscoll, and H. Mitsuya.** 1994. Divergent anti-human immunodeficiency virus activity and anabolic phosphorylation of 2',3'-dideoxynucleoside analogs in resting and activated human cells. J. Biol. Chem. **269**:12633–12638.
10. **Gao, W. Y., T. Shirasaka, D. G. Johns, S. Broder, and H. Mitsuya.** 1993. Differential phosphorylation of azidothymidine, dideoxycytidine, and dideoxyinosine in resting and activated peripheral blood mononuclear cells. J. Clin. Investig. **91**:2326–2333.
11. **Gathe, J. C., Jr., P. Ive, R. Wood, D. Schurmann, N. C. Bellos, E. DeJesus, A. Gladysz, C. Garris, and J. Yeo.** 2004. SOLO: 48-week efficacy and safety comparison of once-daily fosamprenavir /ritonavir versus twice-daily nelfinavir in naive HIV-1-infected patients. AIDS **18**:1529–1537.
12. **HIV Neuromuscular Syndrome Study Group.** 2004. HIV-associated neuromuscular weakness syndrome. AIDS **18**:1403–1412.
13. **Johnson, M., B. Grinsztejn, C. Rodriguez, J. Coco, E. DeJesus, A. Lazzarin, K. Lichtenstein, V. Wirtz, A. Rightmire, L. Odeshoo, and C. McLaren.** 2006. 96-week comparison of once-daily atazanavir/ritonavir and twice-daily lopinavir/ritonavir in patients with multiple virologic failures. AIDS **20**:711–718.
14. **Kodama, E. I., S. Kohgo, K. Kitano, H. Machida, H. Gatanaga, S. Shigeta, M. Matsuoka, H. Ohrui, and H. Mitsuya.** 2001. 4'-Ethynyl nucleoside analogs: potent inhibitors of multidrug-resistant human immunodeficiency virus variants in vitro. Antimicrob. Agents Chemother. **45**:1539–1546.
15. **Koh, Y., H. Nakata, K. Maeda, H. Ogata, G. Bilcer, T. Devasamudram, J. F. Kincaid, P. Boross, Y.-F. Wang, Y. Tie, P. Volarath, L. Gaddis, R. W. Harrison, I. T. Weber, A. K. Ghosh, and H. Mitsuya.** 2003. Novel *bis*-tetrahydrofuranylurethane-containing nonpeptidic protease inhibitor (PI) UIC-94017 (TMC114) with potent activity against multi-PI-resistant human immunodeficiency virus in vitro. Antimicrob. Agents Chemother. **47**:3123–3129.
16. **Maeda, K., K. Yoshimura, S. Shibayama, H. Habashita, H. Tada, K. Sagawa, T. Miyakawa, M. Aoki, D. Fukushima, and H. Mitsuya.** 2001. Novel low molecular weight spirodiketopiperazine derivatives potently inhibit R5 HIV-1 infection through their antagonistic effects on CCR5. J. Biol. Chem. **276**:35194–35200.
17. **Maeda, Y., M. Foda, S. Matsushita, and S. Harada.** 2000. Involvement of both the V2 and V3 regions of the CCR5-tropic human immunodeficiency virus type 1 envelope in reduced sensitivity to macrophage inflammatory protein 1α. J. Virol. **74**:1787–1793.
18. **Masood, R., G. S. Ahluwalia, D. A. Cooney, A. Fridland, V. E. Marquez, J. S. Driscoll, Z. Hao, H. Mitsuya, C. F. Perno, S. Broder, et al.** 1990. 2'-Fluoro-2',3'-dideoxyarabinosyladenine: a metabolically stable analogue of the antiretroviral agent 2',3'-dideoxyadenosine. Mol. Pharmacol. **37**:590–596.
19. **Mitsuya, H., and J. Erickson.** 1999. Discovery and development of antiretroviral therapeutics for HIV infection., p. 751–780. *In* T. C. Merigan, J. G. Bartlet, and D. Bolognesi (ed.), Textbook of AIDS medicine. Williams & Wilkins, Baltimore, MD.
20. **Nakata, H., K. Maeda, T. Miyakawa, S. Shibayama, M. Matsuo, Y. Takaoka, M. Ito, Y. Koyanagi, and H. Mitsuya.** 2005. Potent anti-R5 human immunodeficiency virus type 1 effects of a CCR5 antagonist, AK602/ONO4128/GW873140, in a novel human peripheral blood mononuclear cell nonobese diabetic-SCID, interleukin-2 receptor γ-chain-knocked-out AIDS mouse model. J. Virol. **79**:2087–2096.
21. **Ohrui, H., and H. Mitsuya.** 2001. 4'-C-substituted-2'-deoxynucleosides: a family of antiretroviral agents which are potent against drug-resistant HIV variants. Curr. Drug Targets Infect. Disord. **1**:1–10.
22. **Robbins, B. L., R. V. Srinivas, C. Kim, N. Bischofberger, and A. Fridland.** 1998. Anti-human immunodeficiency virus activity and cellular metabolism of a potential prodrug of the acyclic nucleoside phosphonate 9-*R*-(2-phosphonomethoxypropyl)adenine (PMPA), bis(isopropyloxymethylcarbonyl)PMPA. Antimicrob. Agents Chemother. **42**:612–617.
23. **Siddiqui, M. A., S. H. Hughes, P. L. Boyer, H. Mitsuya, Q. N. Van, C. George, S. G. Sarafinanos, and V. E. Marquez.** 2004. A 4'-C-ethynyl-2',3'-dideoxynucleoside analogue highlights the role of the 3'-OH in anti-HIV active 4'-C-ethynyl-2'-deoxy nucleosides. J. Med. Chem. **47**:5041–5048.
24. **Siliciano, J. D., and R. F. Siliciano.** 2004. A long-term latent reservoir for HIV-1: discovery and clinical implications. J. Antimicrob Chemother. **54**: 6–9.
25. **Simon, V., and D. D. Ho.** 2003. HIV-1 dynamics in vivo: implications for therapy. Nat. Rev. Microbiol. **1**:181–190.
26. **Sosa, N., C. Hill-Zabala, E. DeJesus, G. Herrera, A. Florance, M. Watson, C. Vavro, and M. Shaefer.** 2005. Abacavir and lamivudine fixed-dose combination tablet once daily compared with abacavir and lamivudine twice daily in HIV-infected patients over 48 weeks (ESS30008, SEAL). J. Acquir. Immune Defic. Syndr. **40**:422–427.
27. **Yang, G., G. E. Dutschman, C. J. Wang, H. Tanaka, M. Baba, K. S. Anderson, and Y. C. Cheng.** 2007. Highly selective action of triphosphate metabolite of 4'-ethynyl D4T: a novel anti-HIV compound against HIV-1 RT. Antivir. Res. **73**:185–191.
28. **Yoshimura, K., R. Kato, M. F. Kavlick, A. Nguyen, V. Maroun, K. Maeda, K. A. Hussain, A. K. Ghosh, S. V. Gulnik, J. W. Erickson, and H. Mitsuya.** 2002. A potent human immunodeficiency virus type 1 protease inhibitor, UIC-94003 (TMC-126), and selection of a novel (A28S) mutation in the protease active site. J. Virol. **76**:1349–1358.

AIDS RESEARCH AND HUMAN RETROVIRUSES
Volume 23, Number 3, 2007, pp. 391–397

DOI: 10.1089/aid.2006.0124

# Vpr in Plasma of HIV Type 1-Positive Patients Is Correlated with the HIV Type 1 RNA Titers

SHIGEKI HOSHINO,[1,2] BINLIAN SUN,[1] MITSURU KONISHI,[3] MARI SHIMURA,[1] TATSUYA SEGAWA,[4] YOSHIAKI HAGIWARA,[4] YOSHIO KOYANAGI,[5] AIKICHI IWAMOTO,[6] JUN-ICHI MIMAYA,[7] HIROSHI TERUNUMA,[8] SHIGEYUKI KANO,[1,2] and YUKIHITO ISHIZAKA[1]

## ABSTRACT

**Vpr, an accessory gene product of HIV-1, has been reported in the plasma of HIV-1-positive patients, and exogenous Vpr induces the reactivation of viral production from latently infected cells and the apoptosis of T cells *in vitro*. These observations imply that Vpr is important in AIDS development, but the clinical relevance of the findings cannot be evaluated fully because the actual plasma Vpr concentration in HIV-1-positive patients is unknown. Here we generated two monoclonal antibodies against different portions of Vpr and successfully identified Vpr as a 14-kDa protein in HIV-1-positive patients. Semiquantitative analysis using a recombinant Vpr revealed that the concentration of Vpr in patient plasma was ~0.7 nM (10 ng/ml). Cross-sectional analysis of 52 HIV-1-positive patients revealed that the presence of Vpr detected in 20 patients was positively correlated with HIV-1 RNA copy number ($p < 0.03$), but not with the number of CD4$^+$ T cells. This is the first report demonstrating the actual amount of Vpr in HIV-1-positive patients, and the possible linkage of Vpr and viral titers indicates that it is important to continue to carry out the sequential analysis of Vpr, especially in clinical courses of HIV-1-positive patients. The threshold of viral titers, where Vpr appears in the patients' plasma, if present, contributes to better understanding the role of Vpr in AIDS pathogenesis.**

THE ADOPTION OF ANTIRETROVIRAL THERAPY (ART) has improved the prognosis of HIV-1-positive patients.[1] However, the complete elimination of the virus from patients receiving ART is estimated to take more than 60 years.[2] One factor that may be responsible for this problem is that HIV-1 infects macrophages, latent viral reservoirs[3] from which recurrent viral production is induced by various factors.[4] *Vpr*, an accessory gene of HIV-1, encodes a virion-associated 14-kDa protein that may be critical for the primary infection of macrophages.[5–7] Vpr also induces the reactivation of viral reproduction from latently infected cells. The presence of Vpr in the sera of HIV-1-positive patients, along with the induction of viral reproduction by exogenous Vpr,[8,9] implies that Vpr is actively involved in AIDS development. However, it is necessary to determine the concentration of Vpr in patient plasma samples to correctly evaluate the clinical significance of data obtained from *in vitro* experiments. In the current study, we successfully detected Vpr in patients' samples.

The protocol of this study was approved by the ethics committees of the International Medical Centre of Japan, Nara Medical University, Shizuoka Children's Hospital, and five other hospitals in collaboration with Shizuoka Children's Hospital. Blood plasma samples and peripheral blood were obtained from patients who had given informed consent after the experiment was explained to them. Clinical data on 14 outpatients at Nara Medical University, who were enrolled in the initial study, are

[1]Research Institute, International Medical Center of Japan, Shinjuku-ku, Tokyo 162-8655, Japan.
[2]Graduate School of Comprehensive Human Sciences, University of Tsukuba, Tsukuba 305-8577, Japan.
[3]Center for Infectious Diseases, Nara Medical University, Kashihara, Nara 634-8522, Japan.
[4]Immuno-Biological Laboratories, Co., Fujioka, Gunma 375-0005, Japan.
[5]Laboratory of Viral Pathogenesis, Institute for Virus Research, Kyoto University, Sakyou-ku, Kyoto 606-8507, Japan.
[6]Department of Infectious Diseases, The Institute of Medical Science, The University of Tokyo, Minato-ku 108-8639, Tokyo, Japan.
[7]Department of Hematology and Oncology, Children's Hospital of Shizuoka Prefecture, Aoi-ku, Shizuoka 420-8660, Japan.
[8]Biotherapy Institute of Japan, Koutou-ku, Tokyo, 135-0051, Japan.